Supporting Information

Novel Pathways for Fuels and Lubricants from Biomass Optimized using Life Cycle Greenhouse Gas Assessment

Madhesan Balakrishnan[a], Eric R. Sacia[a,b], Sanil Sreekumar[a], Gorkem Gunbas[a,c], Amit A. Gokhale[a,e], Corinne D. Scown[a,d,1], F. Dean Toste[a,c,1], and Alexis T. Bell[a,b,1]

[a]Energy Biosciences Institute, Berkeley, CA 94720.

[b]Department of Chemical and Biomolecular Engineering, University of California, Berkeley, CA 94720.

[c]Department of Chemistry, University of California, Berkeley, CA 94720.

[d]Energy Technologies Area, Lawrence Berkeley National Laboratory, Berkeley, CA 94720.
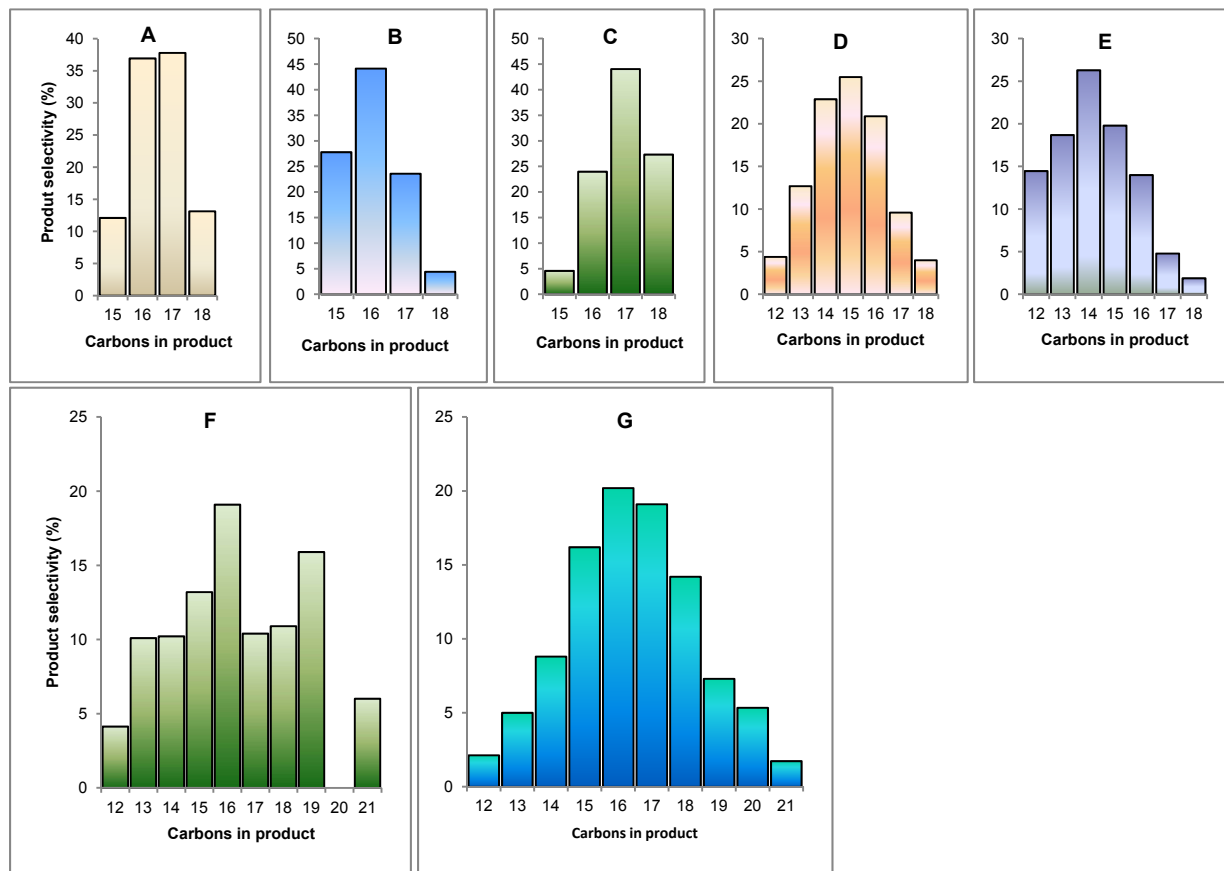
[e]BP North America, Inc.

[1]To whom correspondence should be addressed. E-mail: alexbell@berkeley.edu, fdtoste@berkeley.edu, cdscown@lbl.gov.

1

Contents

1. Additional figures and tables

Fig. S1. MgAlO-catalyzed cross-condensations of mixed ketones and product distributions.

Plot	Ketones (1) and ratios				Selectivities to condensates (3%)									
	$2\text{-}C_4$	$2\text{-}C_5$	$2\text{-}C_6$	$2\text{-}C_7$	C_{12}	C_{13}	C_{14}	C_{15}	C_{16}	C_{17}	C_{18}	C_{19}	C_{20}	C_{21}
A	-	1.00	1.04	-	-	-	-	12	37	38	13	-	-	-
B	-	1.86	1.00	-	-	-	-	28	44	24	4	-	-	-
C	-	1.00	1.90		-	-	-	5	24	44	27	-	-	-
D	1.11	1.07	1.00	-	4	13	23	26	21	10	4	-	-	-
E	2.11	1.07	1.00	-	14	19	26	20	14	5	2	-	-	-
F	1.05	1.00	-	1.04	4	10	10	13	19	10	11	16	-	6
G	1.03	1.00	1.09	1.07	2	5	9	16	20	19	14	7	5	2

Reaction conditions: Mixture of ketones (**1**, 2 mmol in total), MgAlO (200 mg) and toluene (3mL) was heated to 160 °C in a sealed Q-tube reactor for 5 h. $2\text{-}C_4$ = 2-butanone; $2\text{-}C_5$ = 2-pentanone; $2\text{-}C_6$ = 2-hexanone; $2\text{-}C_7$ = 2-heptanone.

Fig. S2. Gas chromatograph traces of (i) C_{12}–C_{18} condensates (Plot D, Fig. S1); (ii) C_{12}–C_{18} alkanes; (iii) C_{12}–C_{21} condensates (Plot G, Fig. S1); (iv) C_{12}–C_{21} alkanes. GC column oven procedure: The column oven was held at 40 °C for three minutes upon injection and then raised at 25 °C/min to 340 °C and held at that temperature for an additional five minutes.

Table S1. A comparison fuel properties of bio-jet fuel with conventional jet fuel (Jet-A).

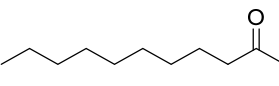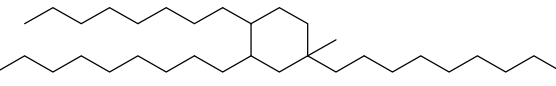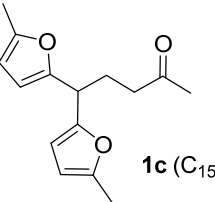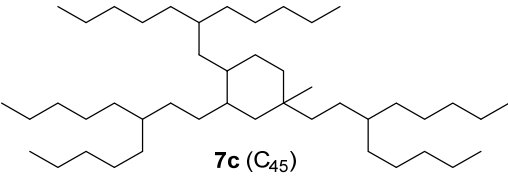| Fuel Property	C_{12} alkanes	$C_{12}–C_{18}$ alkanes	$C_{12}–C_{21}$ alkanes	Conventional jet fuel (Jet-A)
Boiling range (°C)[†]	198–215	198–302	198–339	148–280 (1)
Pour point (°C)[‡]	<-46*	<-46*	<-46*	-
Cloud point (°C)[#]	<-54*	<-54*	<-54*	-
Freeze point (°C)[⊥]	<-100*	<-100*	<-100*	-40**
ΔH_{comb} (MJ L^{-1})	38.3	38.3	38.8	36.1 (1)
$\rho_{25°C}$ (g mL^{-1})	0.815	0.813	0.82	0.805 (1)
DCN	-	-	48.6	-

[†]ASTM standard D2887 and D86; [‡]ASTM standard D7346; [#]ASTM standard D5772; [⊥]ASTM standard D7153; *These measurements exceeded the measurement range of the equipment by the ASTM standards; **Specification from ASTM D1655; ΔH_{comb} = energy density; $\rho_{25°C}$ = density at 25 °C; DCN = derived cetane number.

Table S2. Bio-lubricants (**7a–c**) and characteristics.

Entry	Ketone (1)	Lubricant (7)	Viscosity Index (VI)	Pour Point (°C)
1	**1a** (C_{11})	**7a** (C_{33})	66	-54
2	**1b** (C_{11})	**7b** (C_{33})	123	-69
3	**1c** (C_{15})	**7c** (C_{45})	94	-51
4†	-	PAO4	124	-72
5‡	-	Group I base oils	80 to 120	-15 to -30

Literature reports: †(2), ‡(3).

2. Experimental procedures

General:

Materials: Chemicals were used as received without further purification. Commercially available ketones, 2-methylfuran and octane were purchased from Sigma-Aldrich, USA. All HPLC grade solvents, such as acetone, acetonitrile, dichloromethane, diethyl ether, ethyl acetate, hexanes, tetrahydrofuran and toluene were obtained from Fisher Scientific, USA. Anhydrous inorganic solids (Na_2CO_3, Na_2SO_4 and $MgSO_4$) were purchased from Fisher Scientific, USA. Catalysts and metal precursors such as synthetic hydrotalcite and chloroplatinic acid hexahydrate were obtained from Sigma-Aldrich, USA. Niobium based catalysts including niobic acid and niobium phosphate were received in kind from CBMM, Brazil. 2 wt% $Pt/NbOPO_4$ was synthesized according to the procedure from the literature report (4). Ketones **1a** (5) and **1c** (6) were synthesized using literature procedures.

Methods: Reaction mixtures were analyzed using a Varian CP-3800 gas chromatograph (GC) equipped with a flame ionization detector (FID) coupled to a Varian 320-MS mass spectrometer (MS). Products were separated using a FactorFour capillary column (VF-5 ms, 30 m length, 0.25 mm diameter) coated with a 0.25 µm thick stationary phase (5% phenyl and 95% dimethylpolysiloxane). Products identified by GC/MS were also confirmed by NMR experiments of chromatographically purified authentic samples. These authentic samples were used to develop calibration curves using dodecane as an internal standard for quantitative analysis of reaction mixtures by GC/FID.

a. Preparation of catalysts and characterization

MgAlO: The commercial synthetic hydrotalcite (Mg/Al = 3:1) was calcined at 700 ºC for 2 h in static air by ramping at 2 ºC/min.
Nb_2O_5: The commercial niobic acid was calcined at 300 ºC for 3 h in a tubular oven by ramping at 2 ºC/min. An air flow was maintained at 50 mL/min throughout the course of calcination.
2 wt% $Pt/NbOPO_4$: The commercial niobium phosphate was calcined as mentioned above for Nb_2O_5. Chloroplatinic acid hexahydrate (212 mg) was dissolve in deionized water (1 mL) and impregnated on calcined niobium phosphate (4 g) using the incipient wetness method. This material was dried overnight in an oven at 100 °C and subjected to reduction at 300 ºC for 3 h in a tubular oven by ramping at 2 ºC/min. The hydrogen flow (9% in He) was maintained at 50 mL/min throughout the course of reduction.

Surface area measurements: Catalyst surface area was determined by Brunauer-Emmett-Teller (BET) analysis using a Micromeritics TriStar system with a FlowPrep 060 degassing system. The material (~200 mg) was degassed in a BET tube at 120°C for 6 hours under flowing argon. The catalyst surface area was determined by the BET isotherm. The surface area for MgAlO,

Nb_2O_5, and $Pt/NbOPO_4$ catalysts were found to be 174 ± 2, 105.0 ± 0.4, and 157 ± 1 m^2/g, respectively.

Pt dispersion measurement: CO pulse chemisorption was used to measure particle size and dispersion of Pt nanoparticles on the $Pt/NbOPO_4$ catalyst using a Micromeritics AutoChem II Chemisorption Analyzer. Approximately 125 mg of catalyst was added to the sample tube and reduced in 10% H_2 in Ar for 30 minutes at 250°C (10°C/min temperature ramp). The catalyst was then cooled to 40°C and CO pulses were used to titrate surface metal sites until no change was observed in CO adsorption. In this way, the dispersion of Pt on $NbOPO_4$ was found to be 13.4% (8.4 nm particles).

X-ray Diffraction of Catalyst Solids

Catalyst powder patterns were analyzed using x-ray diffraction (XRD) to assess the crystallographic structure of each solid catalyst. These measurements were made on a Bruker D8 instrument over a 2θ range of 10-80 degrees or 20-60 degrees using a step size of 0.02 degrees.
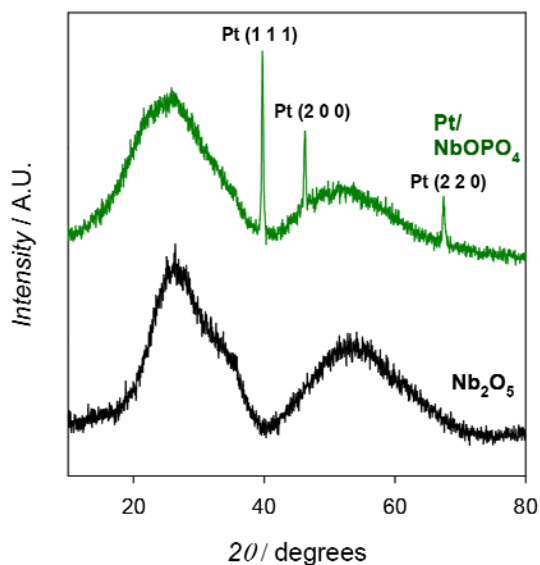

Fig. S3. XRD powder patterns of Nb_2O_5 and $Pt/NbOPO_4$ (2 wt%). Peaks relevant to Pt nanoparticles can clearly be observed by XRD.
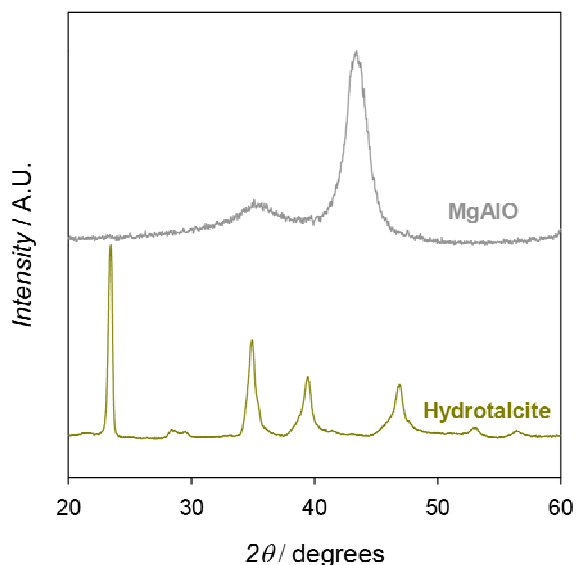
Fig. S4. XRD powder patterns of as-received hydrotalcite, which forms a brucite-like structure, and calcined hydrotalcite (MgAlO), which forms a disordered structure with some cubic characteristics.

b. Syntheses of Jet fuels and Lubricants

(i) Condensation of ketones (1): Q-tube reactions for qualitative/quantitative analysis

A solution of **1** (2 mmol) in toluene (3 mL) was added with catalyst (200 mg, MgAlO/Nb_2O_5) in a Q-tube equipped with a magnetic spin bar. The reaction mixture was sealed using PTFE-coated rubber seals and magnetically stirred (800 rpm) in a pre-heated oil bath under the conditions listed in Table 1. The reaction mixture was then cooled, and an internal standard (dodecane) was added. The product mixture was then passed through a small plug of silica gel and washed with ethyl acetate (3×10 mL) to remove solid catalyst particles. The crude products (**2–5**) in the filtrate were then analyzed/quantified using gas chromatography.

(ii) Condensation of ketones: Dean-Stark reactions for large-scale synthesis of C$_{12}$, C$_{12}$–C$_{18}$, and C$_{12}$–C$_{21}$ jet fuel condensates (3)

A solution of **1** (180 mmol) in toluene (200 mL) was added with MgAlO (16 g) in a 500 mL round bottom flask (RBF) equipped with a magnetic spin bar. The RBF was then attached to the Dean-Stark apparatus and refluxed with stirring (800 rpm) in a pre-heated oil bath at 160 ˚C for 6 hours. The by-product water was continuously removed from the reaction mixture and collected in the side-arm of the apparatus during the course of the reaction. The product mixture was then cooled to room temperature and filtered through a fritted funnel by washing the catalyst using ethyl acetate (3×100 mL). The products (**3**) in the filtrate were recovered after evaporation of the solvents.

(iii) Condensation of ketones: Dean-Stark reactions for large-scale synthesis of C_{33} and C_{45} lubricant condensates (3a–c)

The above procedure was followed except the reflux was continued for 16 h.

(iv) Solvent-free self-condensation of 2-heptanone

250ml RBF was charged with 10-15g of hydrotalcite (calcined at 700 ºC, 2hrs, 2 ºC /min ramp), ~50-60g of 2-heptanone, and a large stir bar. An empty Dean-Stark trap and condenser were added to the flask, and the apparatus was heated to reaction temperature with stirring (800 rpm) using a high-temperature oil bath. The reaction was allowed to proceed for eight hours. The reaction mixture was allowed to cool to RT and settle, then a 0.5ml aliquot of supernatant was withdrawn and dissolved in toluene for analysis by GC-FID. The GC-FID showed that the isomers of the trimer were the only products produced.

Entry	Reactant:Catalyst g/g	Temperature (ºC)	Time (min)	Yield
1	5.61	160	300	29.1%
2	5.91	210	30	26.5%
3	5.90	210	60	70.5%
4	5.95	210	90	100%

(v) General procedure for alkylation of acetone

A 12 mL Q-tube containing a stir bar and 2 wt% Pd/MgAlO (1.7 mol%, 350 mg) was charged with an equimolar solution of acetone and the respective alcohol. The Q-tube was sealed and the reaction mixture was stirred at conditions mentioned below in a pre-heated metal block. The reaction mixture was cooled to room temperature and dodecane (internal standard) was added. The reaction mixture was diluted with tetrahydrofuran and the GC analysis of the reaction mixture was carried out.

Alcohol	T (°C)	Time (h)	Conversion (%)	Product selectivity (%)	
				Monoalkylation	Dialkylation
ethanol	250	0.25	100	67 (2-pentanone)	33 (4-heptanone)
1-butanol	250	0.25	100	67 (2-heptanone)	33 (6-undecanone)
1-octanol	200	24	44	87 (2-undecanone)	13 (10-nonadecane)

(vi) Hydrodeoxygenation of condensates (3) to alkanes (7):

A solution of **3** (5 mmol) in octane (5 mL) was added with 2 wt% Pt/NbOPO$_4$ (120 mg, 0.25 mol% Pt with respect to **3**) in a 25 mL Parr reactor vessel. The reactor was sealed, flushed with 3.5 MPa of nitrogen gas (2×), hydrogen gas (3×) and subsequently charged with the required pressure of hydrogen gas. The Parr reactor was stirred at 500 rpm and subjected to respective

conditions listed below. The reaction mixture was cooled to room temperature and filtered through a fritted funnel using hexanes as a washing solvent (3×20 mL) to remove the catalyst. The crude products in the filtrate were then analyzed/quantified using gas chromatography. The filtrate was concentrated under reduced pressure to recover cyclic alkanes.

Jet fuel condensates **3**: 3.5 Mpa of H_2, 160 ºC, 5 h.

Lubricant condensates **3a** and **3b**: 3.5 Mpa of H_2, 160 ºC, 12 h.

Lubricant condensate **3c**: Because of the presence of furan moieties, hydrodeoxygenation was performed in two stages. 10 wt% Pd/C (13 mg, 0.25 mol%), 2.1 MPa, 100 ºC, 3 h and then 2 wt% Pt/NbOPO$_4$ (240 mg, 0.5 mol% Pt), 3.5 Mpa of H_2, 250 ºC, 5 h.

c. Determination of Heat of Combustion Value for Jet fuels

Values for heat of combustion were determined using standard methods for bomb calorimetry available from Parr Instrument Company in manuals 204M and 205M and in ASTM D4809. The Parr 1108 bomb calorimeter was calibrated using a benzoic acid standard (~1g, Parr item: 3413) and Parr 45C10 fuse wire (2.3 cal/cm).

The calorimeter system temperature was measured using LabVIEW. For the C_{12} alkane, Parr gelatin capsules (Parr item: 3601) containing approximately 0.9 mL of fuel were combusted in 30 atm of oxygen. Benzoic acid, the C_{12} alkane jet fuel, and empty Parr capsules were run twice in each case to establish reproducibility.

d. Method of Simulated Distillation for Jet fuels

A simulated distillation is achieved by correlating boiling point to gas chromatograph (GC) retention time during a linearly-ramped GC program. This procedure is similar to the established procedures given in ASTM D2887. The samples were run on a Varian CP-3800 GC equipped with a flame ionization detector (FID) and a Varian factorFOUR capillary column (30 m, 0.25 mm diameter). The column oven was held at 35 °C for three minutes upon injection and then raised at 10 °C/min to 300 °C and held at that temperature for an additional five minutes.

A standard mixture of 1 mg/mL *n*-heptane through icosane in dichloromethane was then injected in this method to correlate retention time to each alkane's boiling point (Fig. S5). The jet fuel sample to be evaluated was then injected. The fraction of the mixture's mass that corresponded to each boiling temperature could then be ascertained to provide the previously shown figure for the simulated distillation.
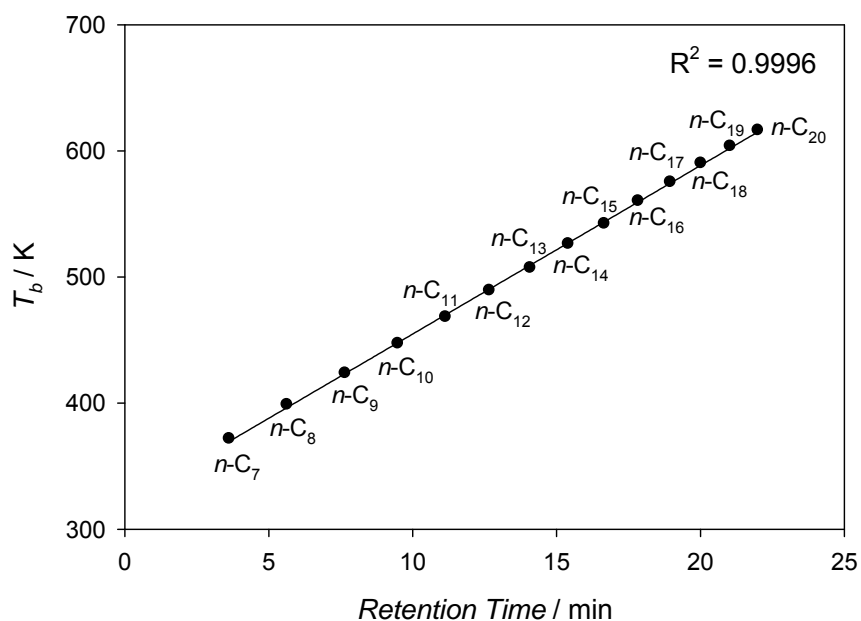
Fig. S5. Correlation of boiling point (T_b) with GC retention time for C_7–C_{20} n-alkanes.

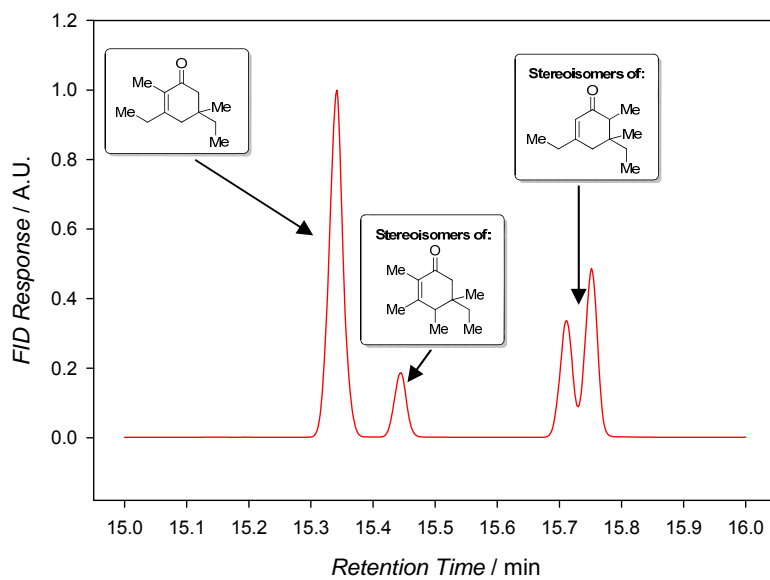## 3. Characterization of condensates (3), fuels (7), and lubricants (7a–c)

Fig. S6. Gas chromatograph trace of the products of 2-butanone trimerization.
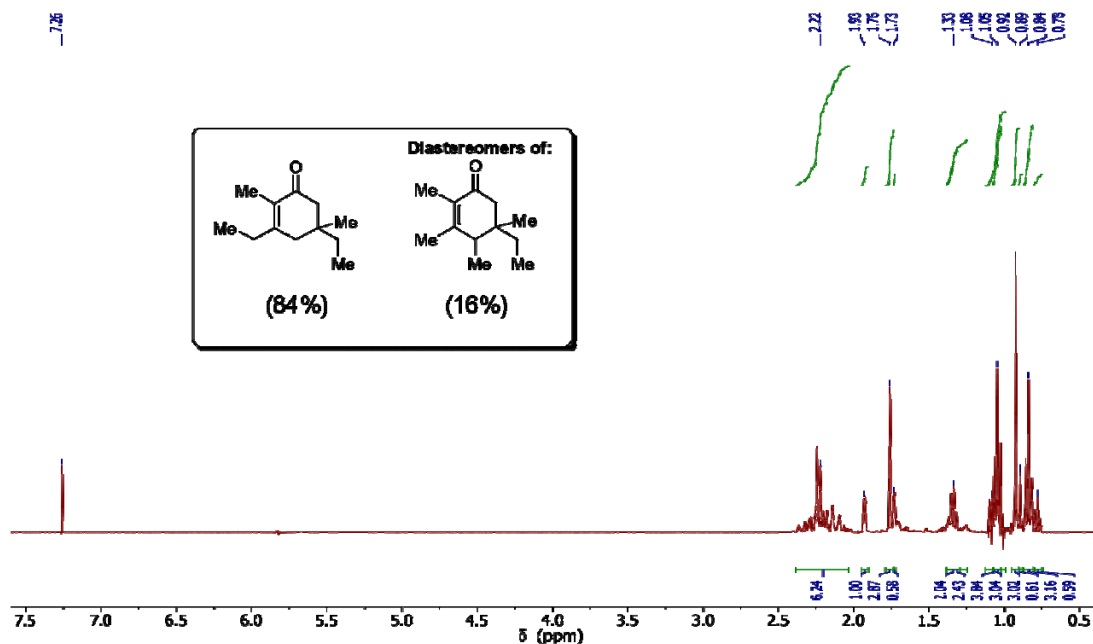
11

Fig. S7. ¹H NMR of products of 2-butanone trimerization. Major product: ¹H NMR (400 MHz, Chloroform-d) δ 2.37-2.05 (m, 5H), 1.93 (d, *J* = 4.4 Hz, 1H), 1.76 (bs, 3H), 1.34 (q, *J* = 7.2 Hz, 2H), 1.05 (t, *J* = 7.6 Hz, 3H), 0.92 (s, 3H), 0.84 (t, *J* = 7.6 Hz, 3H). Minor product: δ 2.37-2.05 (m, 6H), 1.73 (bs, 3H), 1.38-1.22 (m, 2H), 1.07 (d, *J* = 7.0 Hz, 3H), 0.89 (s, 3H), 0.78 (t, *J* = 7.6 Hz, 3H).
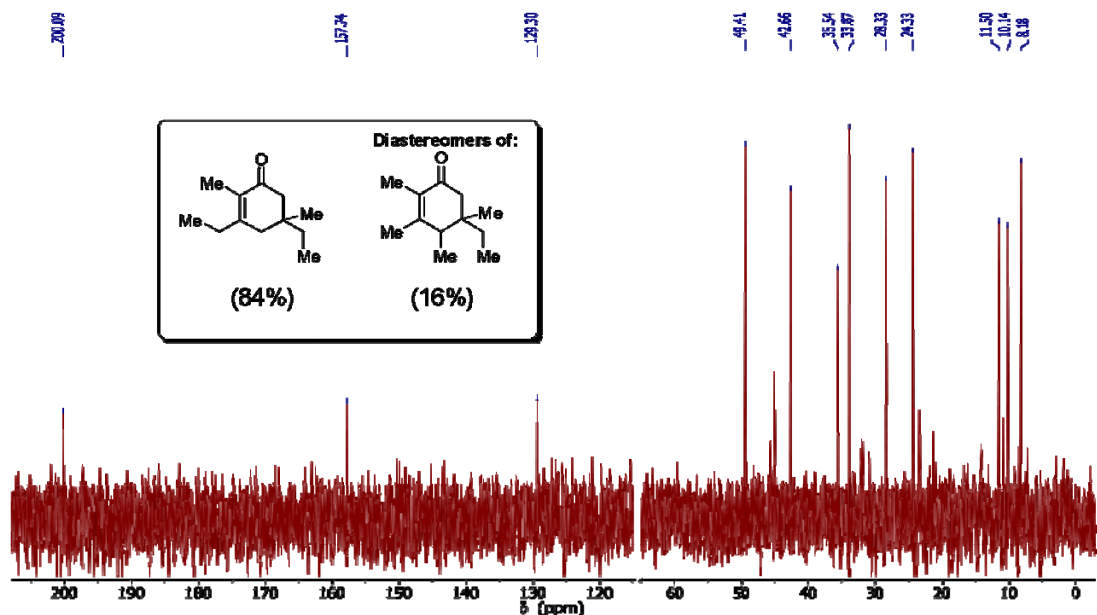

Fig. S8. ¹³C NMR of a single isomer product of 2-butanone trimerization. Major product: ¹³C NMR (101 MHz, Chloroform-d) δ 200.1, 157.7, 129.3, 49.4, 42.7, 35.5, 33.9, 28.3, 24.3, 11.5, 10.1, 8.2.
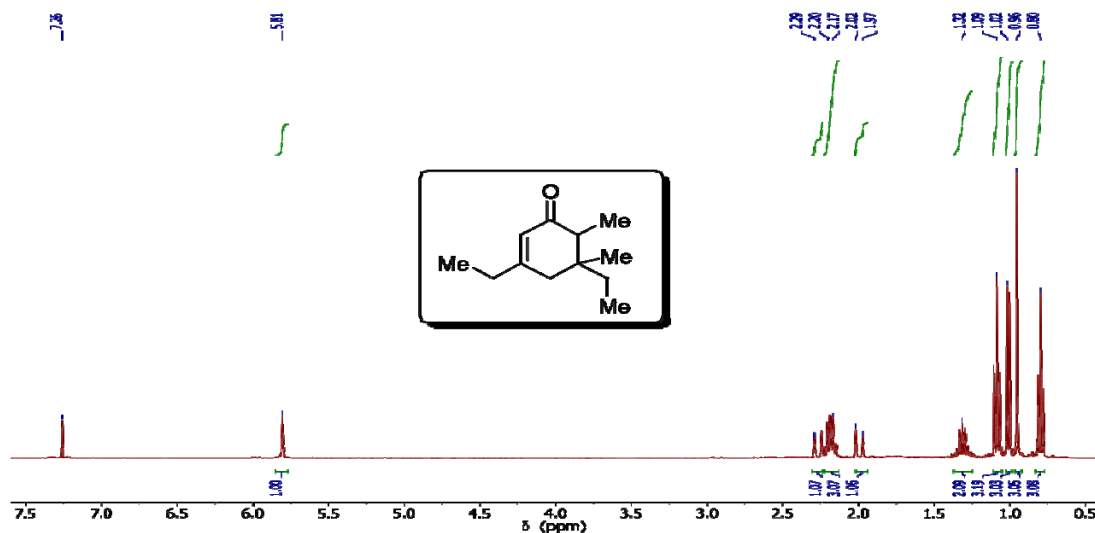
12

Fig. S9. ¹H NMR of a single isomer product of 2-butanone trimerization. ¹H NMR (400 MHz, Chloroform-d) δ 5.81 (p, J = 1.5 Hz, 1H), 2.27 (d, J = 18.3 Hz, 1H), 2.20 (q, J = 7.2 Hz, 1H), 2.18 (q, J = 7.6 Hz, 2H), 2.00 (d, J = 18.4 Hz, 1H), 1.31 (dq, J = 13.8, 7.1, 6.6 Hz, 2H), 1.09 (t, J = 7.4 Hz, 3H), 1.01 (d, J = 7.2 Hz, 3H), 0.96 (s, 3H), 0.80 (t, J = 7.5 Hz, 3H).
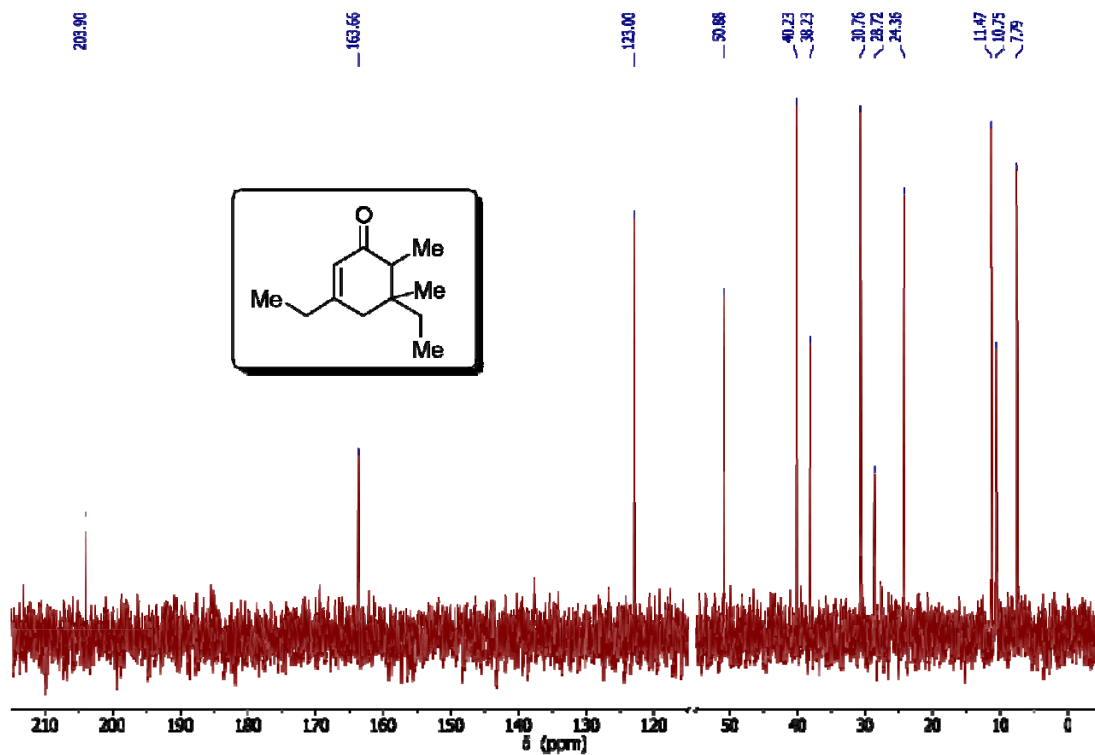

Fig. S10. ¹³C NMR of a single isomer product of 2-butanone trimerization. ¹³C NMR (101 MHz, Chloroform-d) δ 203.9, 163.7, 123.0, 50.9, 40.2, 38.2, 30.8, 28.7, 24.4, 11.5, 10.8, 7.8.
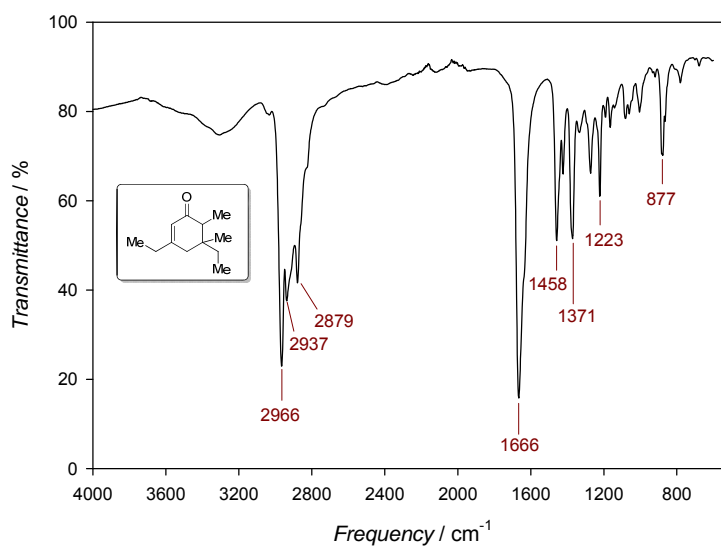
13

Fig. S11. FTIR-ATR of a single isomer product of 2-butanone trimerization. A characteristic cyclic enone stretch is observed at 1666 cm^{-1}.
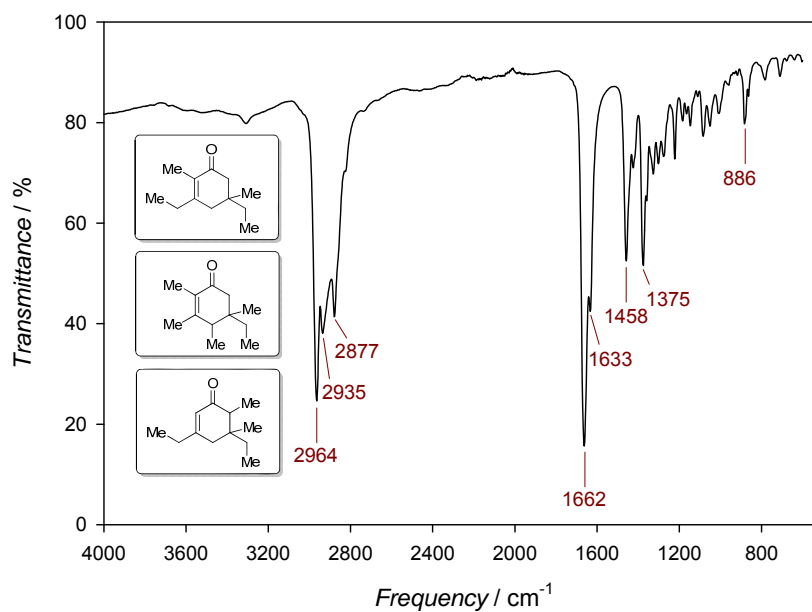
Fig. S12. FTIR-ATR of the mixture of isomers of 2-butanone trimerization. The characteristic cyclic enone stretch is observed at 1662 cm^{-1}.
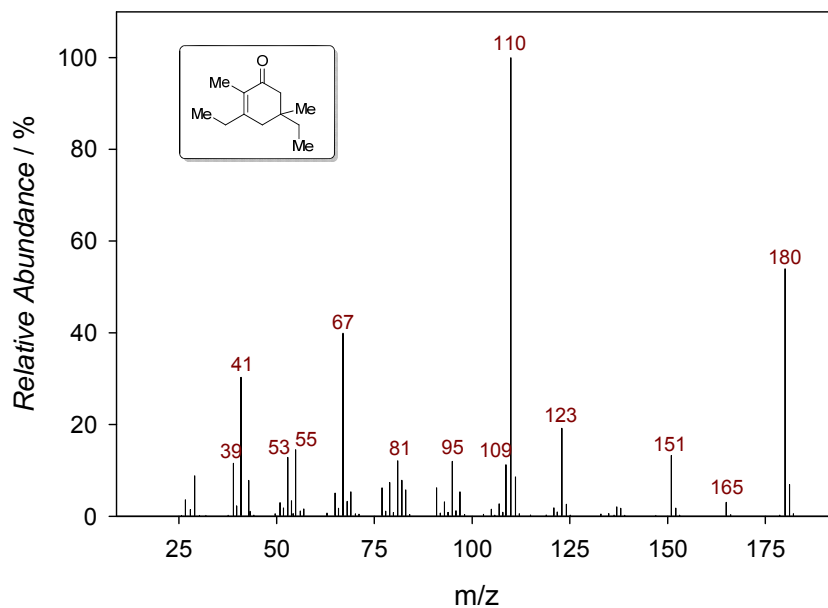
Fig. S13. Mass spectra of a single isomer product of 2-butanone trimerization.
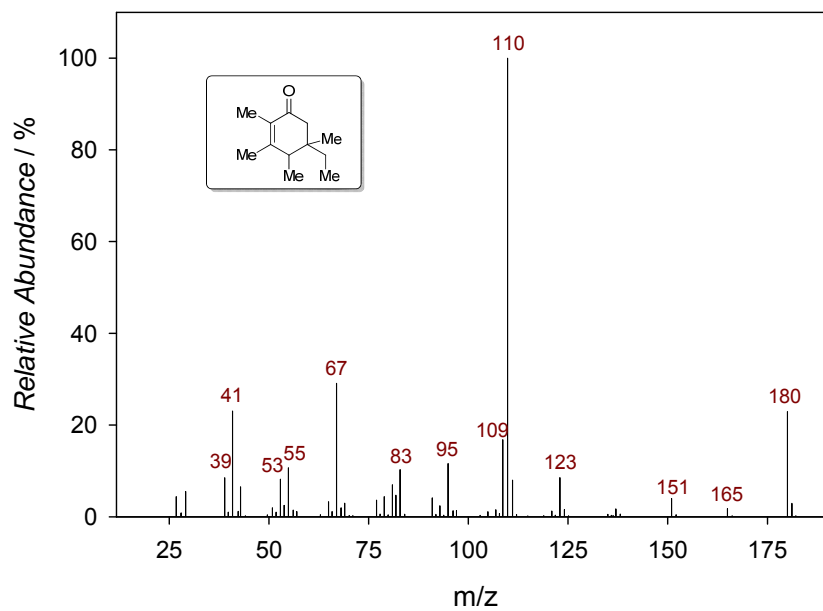
Fig. S14. Mass spectra of a single isomer product of 2-butanone trimerization.

15
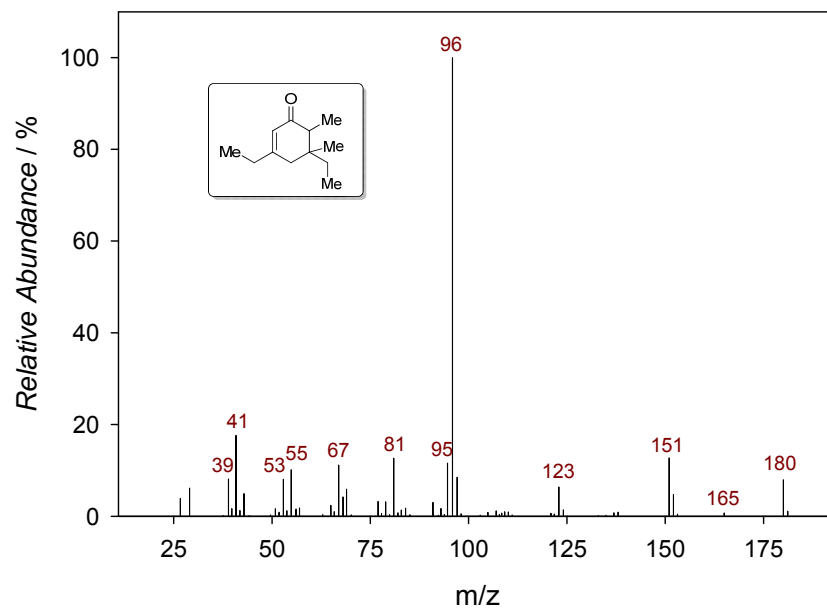
Fig. S15. Mass spectra of a single isomer product of 2-butanone trimerization.
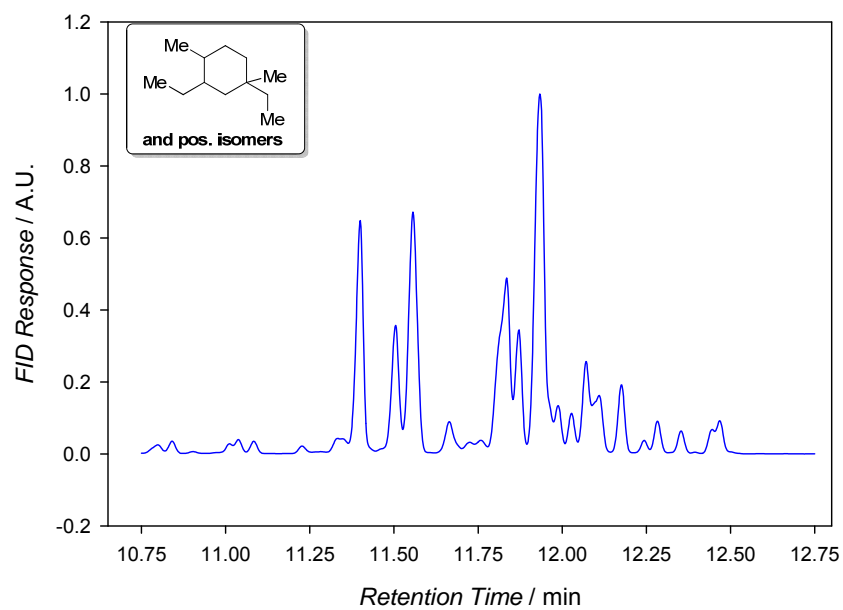
Fig. S16. Gas chromatograph trace of the C_{12} products of 2-butanone trimerization and hydrodeoxygenation.

Fig. S17. Proton NMR of 2-butanone trimers after hydrodeoxygenation. ^{1}H NMR (400 MHz, Chloroform-d) δ 1.90-0.50 (m).
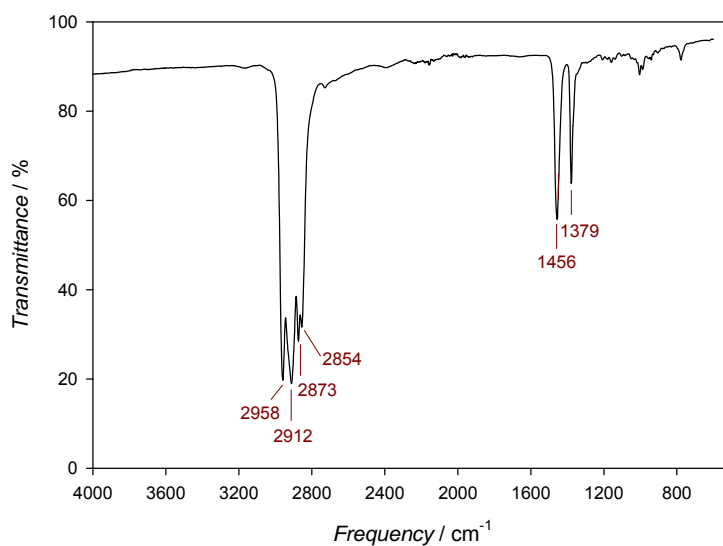
Fig. S18. FTIR-ATR of 2-butanone trimers after hydrodeoxygenation.

17
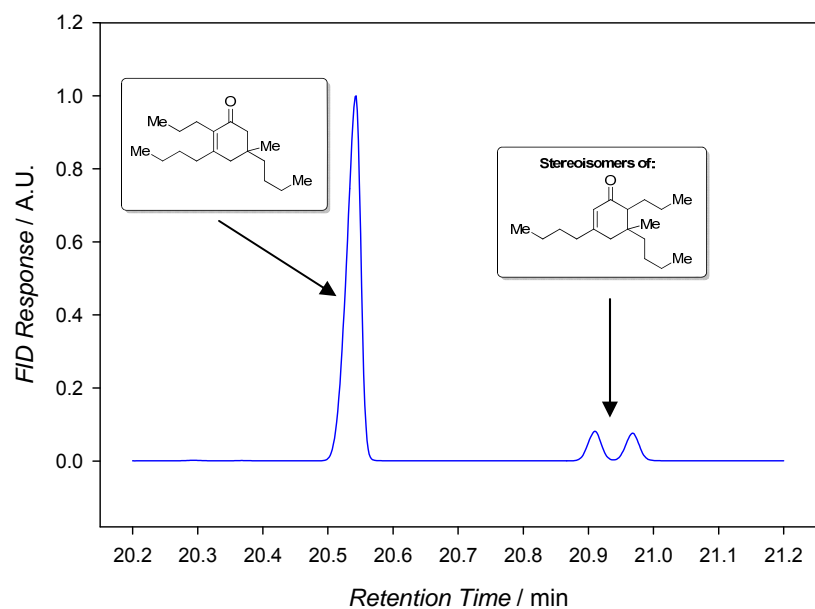
Fig. S19. Gas chromatograph trace of the products of 2-hexanone trimerization.
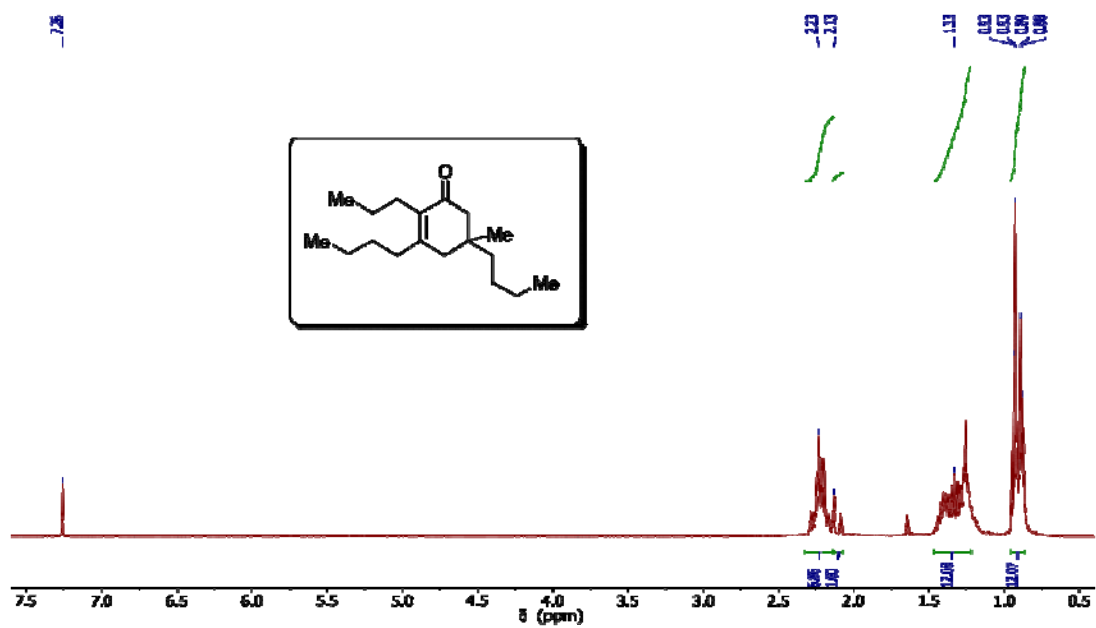
Fig. S20. ^{1}H NMR of a single isomer product of 2-hexanone trimerization. ^{1}H NMR (400 MHz, Chloroform-d) δ 2.28-2.15 (m, 7H), 2.11 (d, J = 18.0 Hz, 1H), 1.46-1.19 (m, 12H), 0.93 (t, J = 7.2 Hz, 3H), 0.93 (s, 3H), 0.89 (t, J = 7.4 Hz, 3H), 0.88 (t, J = 6.8 Hz, 3H).
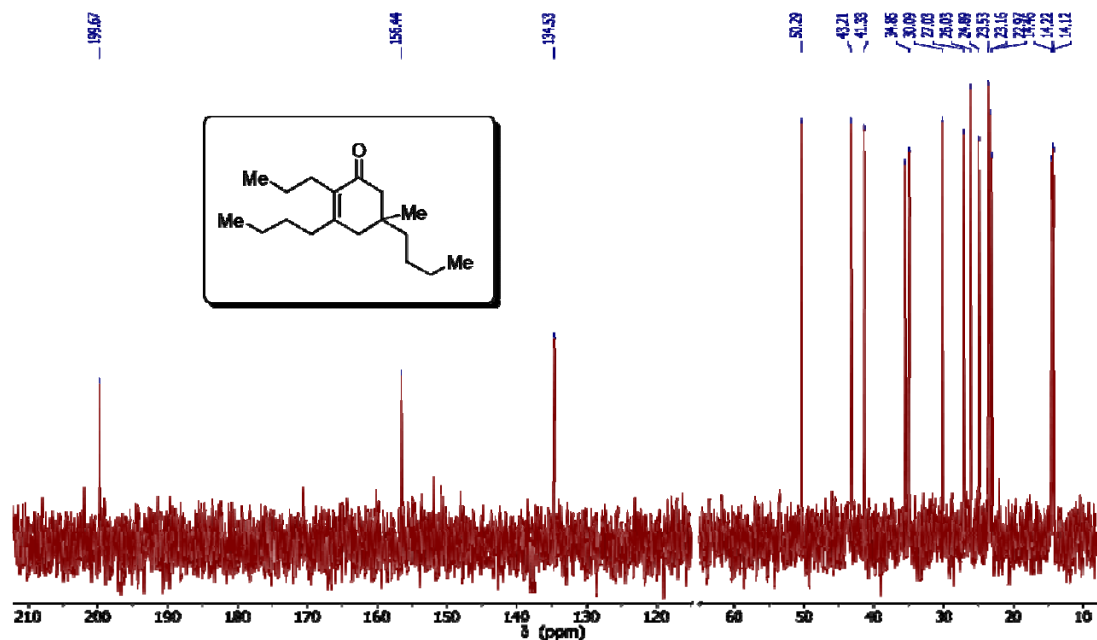
Fig. S21. ^{13}C NMR of a single isomer product of 2-hexanone trimerization. ^{13}C NMR (101 MHz, Chloroform-d) δ 199.7, 156.4, 134.5, 50.3, 43.2, 41.3, 35.5, 34.9, 30.1, 27.0, 26.0, 24.9, 23.5, 23.2, 23.0, 14.5, 14.2, 14.1.
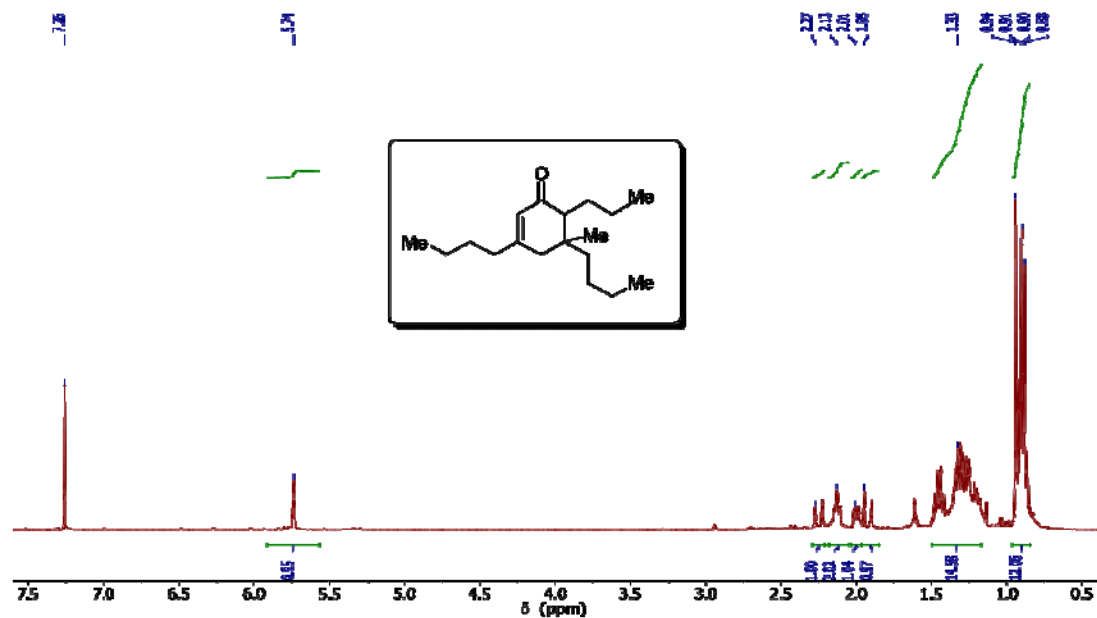
Fig. S22. ^{1}H NMR of a single isomer product of 2-hexanone trimerization. ^{1}H NMR (400 MHz, Chloroform-d) δ 5.74 (bs, 1H), 2.25 (d, J = 18.4 Hz, 1H), 2.13 (td, J = 7.2, 2.9 Hz, 2H), 2.00 (dd, J = 10.2, 3.4 Hz, 1H), 1.93 (d, J = 18.4 Hz, 1H), 1.48-1.15 (m, 14H), 0.94 (s, 3H), 0.91 (t, J = 7.2 Hz, 3H), 0.90 (t, J = 7.2 Hz, 3H), 0.88 (t, J = 6.8 Hz, 3H).

19
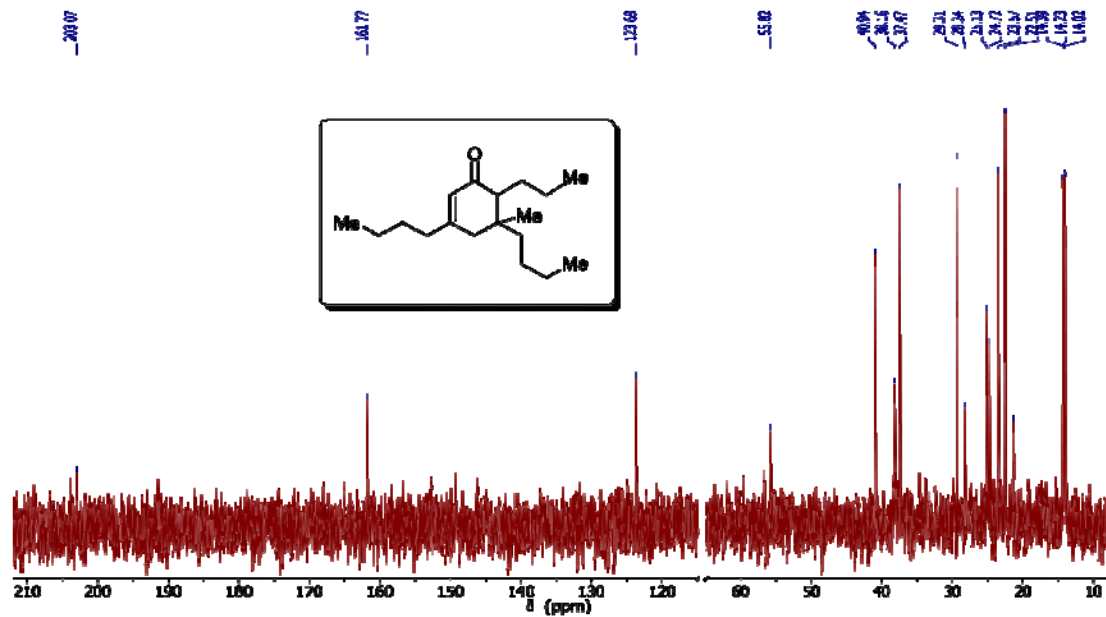
Fig. S23. ^{13}C NMR of a single isomer product of 2-hexanone trimerization. ^{13}C NMR (101 MHz, Chloroform-d) δ 203.1, 161.8, 123.7, 55.8, 40.9, 38.2, 37.5, 29.3, 28.2, 25.1, 24.7, 23.6, 22.5, 21.4, 14.4, 14.2, 14.0.
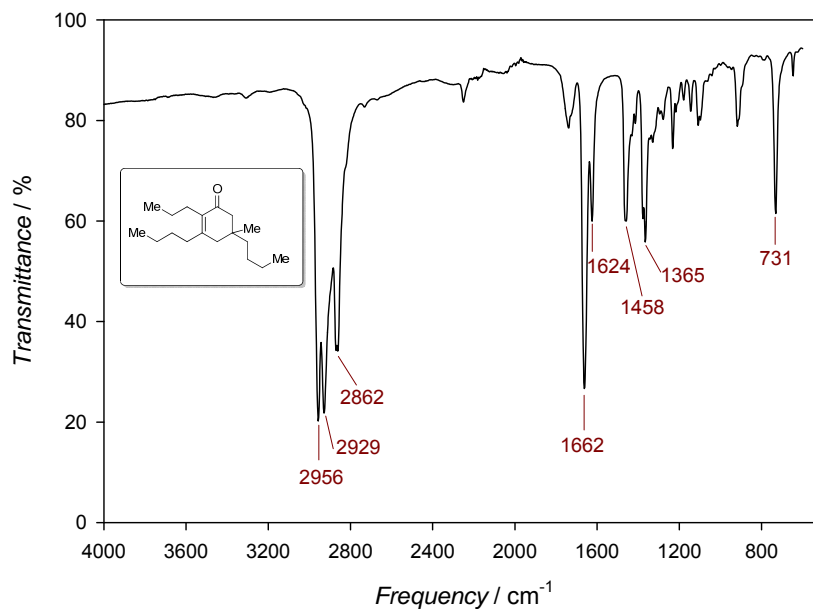
Fig. S24. FTIR-ATR of a single isomer product of 2-hexanone trimerization. A characteristic cyclic enone stretch is observed at 1662 cm^{-1}.
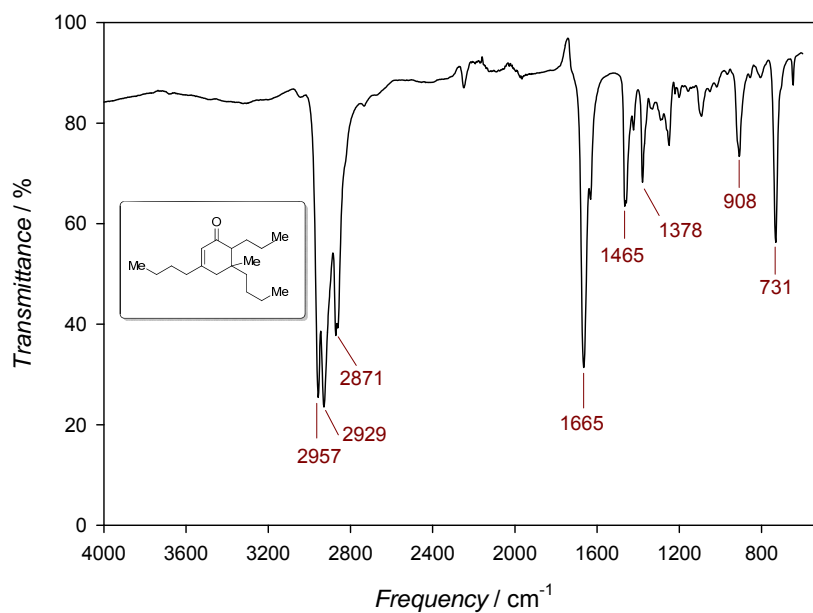
Fig. S25. FTIR-ATR of a single isomer product of 2-hexanone trimerization. A characteristic cyclic enone stretch is observed at 1665 cm^{-1}.
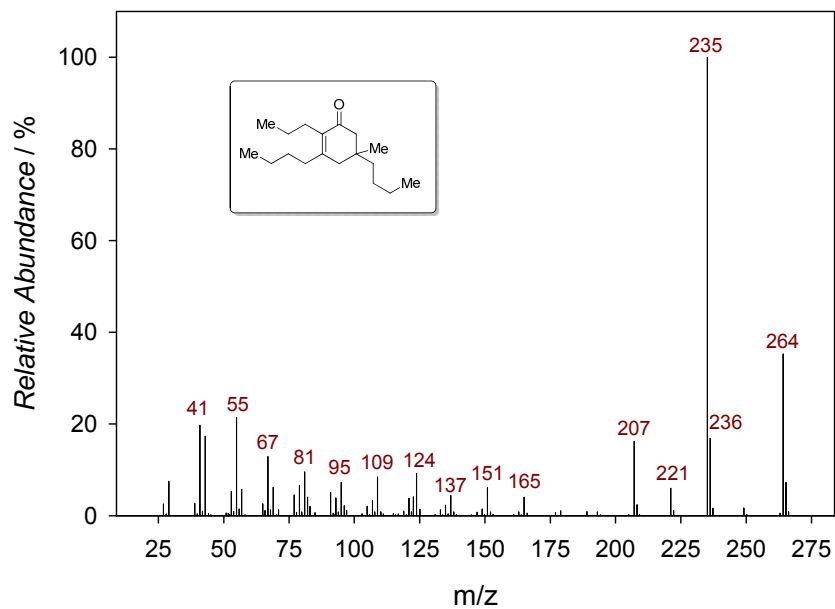
Fig. S26. Mass spectra of a single isomer product of 2-hexanone trimerization.
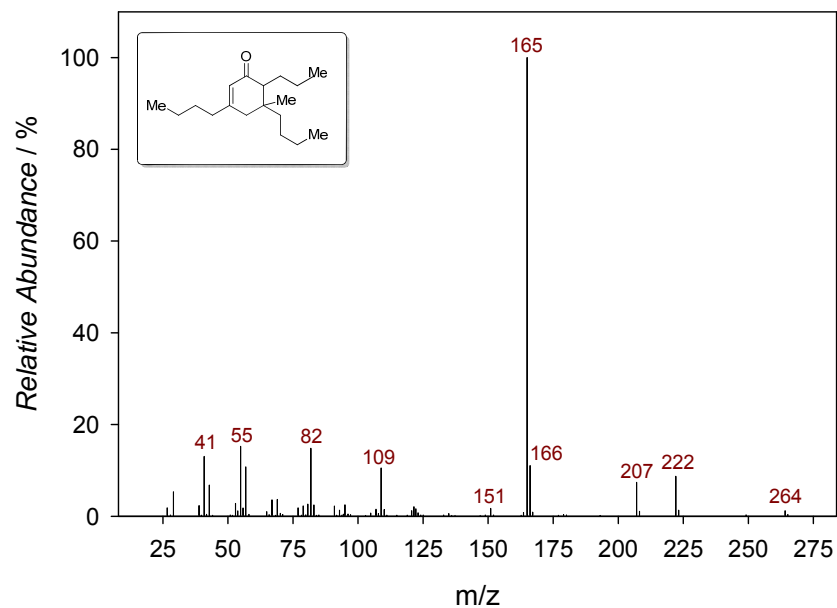
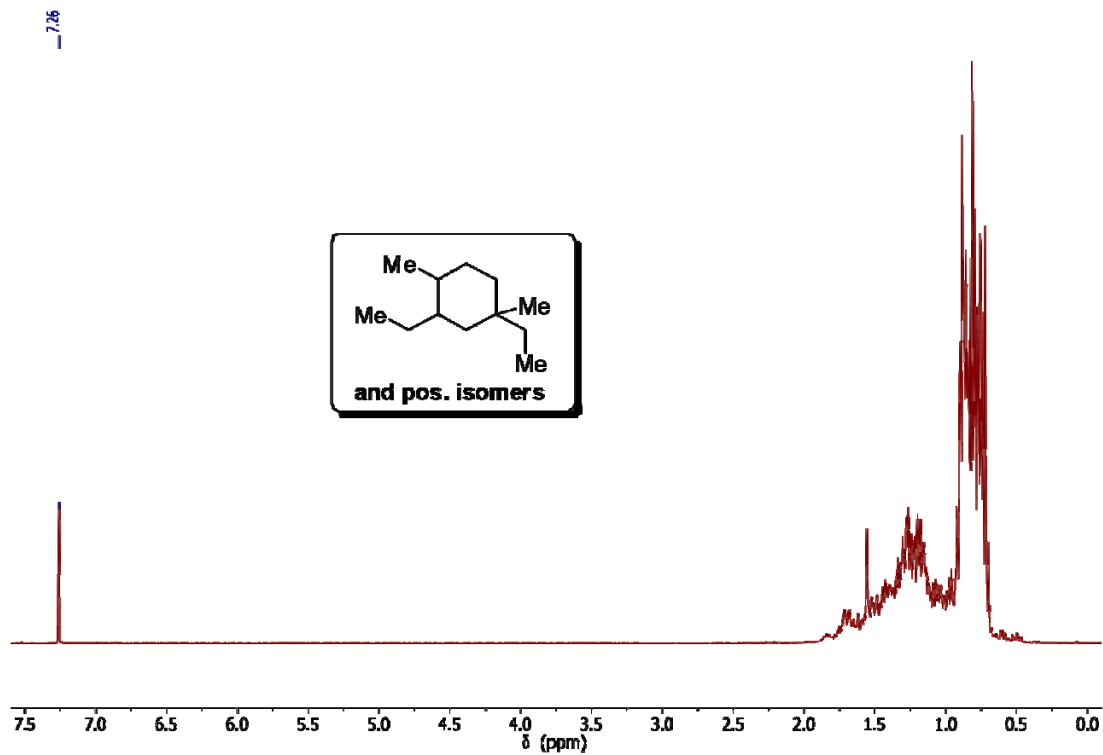**Fig. S27.** Mass spectra of a single isomer product of 2-hexanone trimerization.
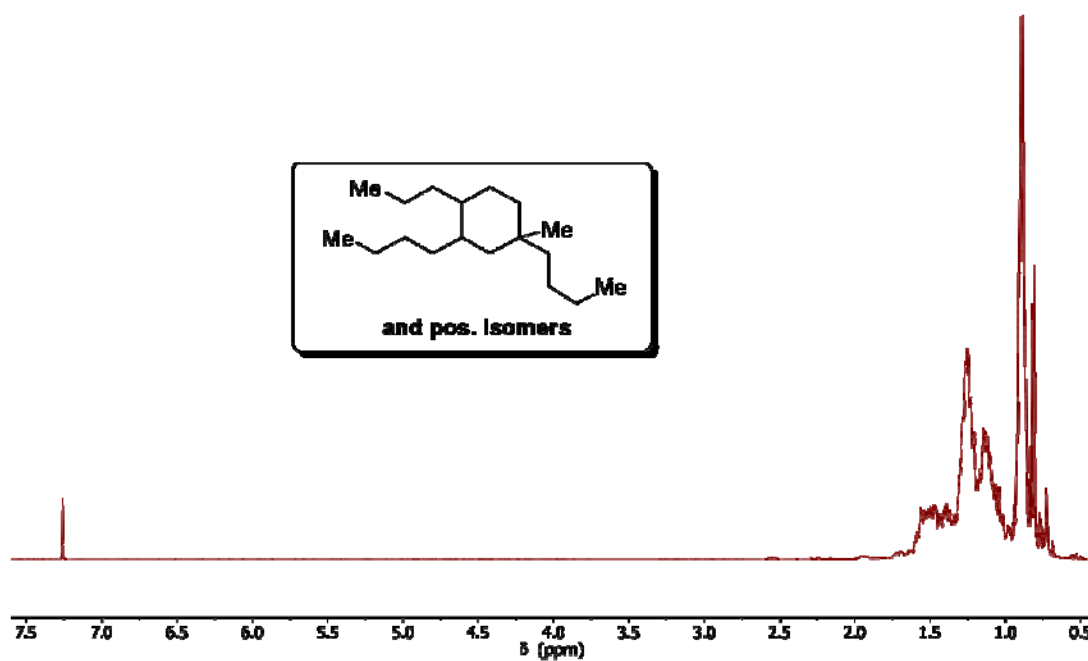
Fig. S28. Proton NMR of 2-hexanone trimers after hydrodeoxygenation. ^{1}H NMR (400 MHz, Chloroform-d) δ 1.80-0.60 (m).
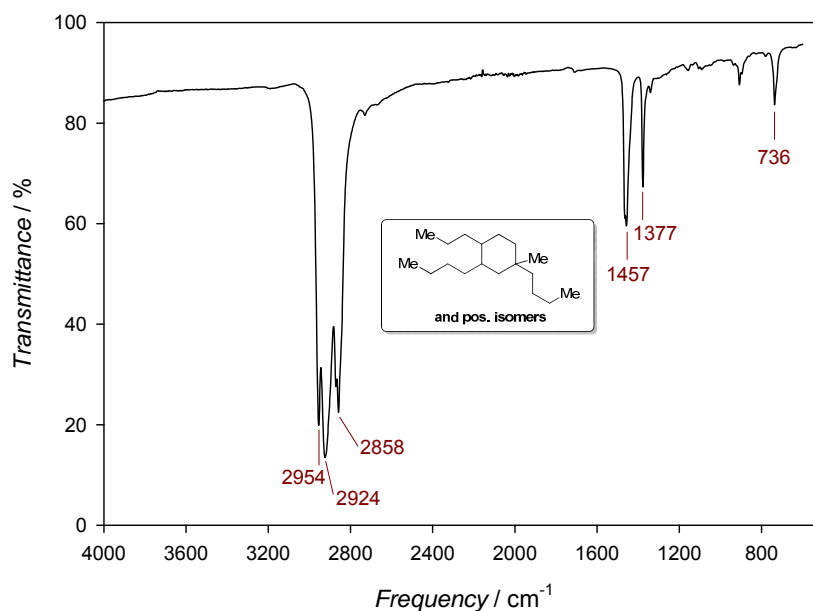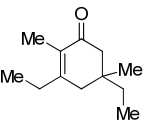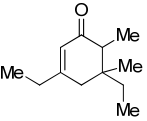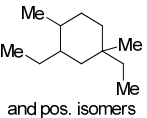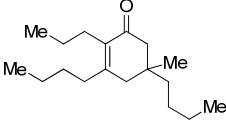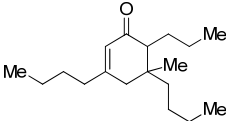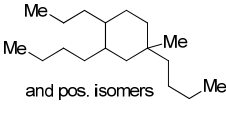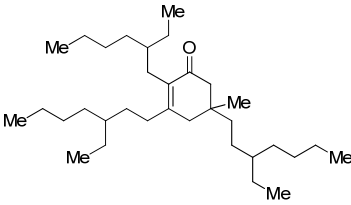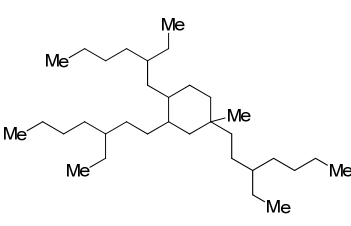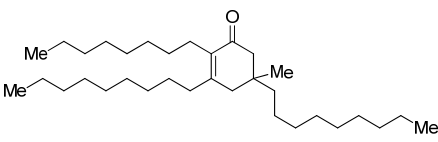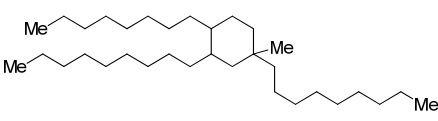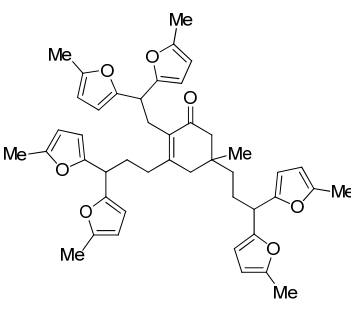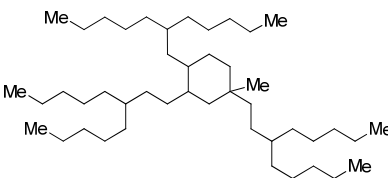
**Fig. S29.** FTIR-ATR of 2-hexanone trimers after hydrodeoxygenation.

High Resolution Mass Spectrometry Characterization

Monoisotopic masses of several major products were collected in coordination with QB3/Chemistry Mass Spectrometry Facility at the University of California, Berkeley. Individual products were confirmed by high-resolution mass spectrometry (HRMS) using a magnetic sector mass spectrometer (AutoSpec Premier) and EI ionization. The monoisotopic masses (expected vs. measured) and the coordinating molecular formula are listed in Table S3.

Table S3. HRMS Characterization data for key compounds

Molecular Structure	Molecular Formula	Expected Monoisotopic Mass	Measured Monoisotopic Mass
	$C_{12}H_{20}O$	180.1514	180.1514
	$C_{12}H_{20}O$	180.1514	180.1516
	$C_{12}H_{24}$	168.1878	168.1874

23

	$C_{18}H_{32}O$	264.2453	264.2451
	$C_{18}H_{32}O$	264.2453	264.2446
	$C_{18}H_{36}$	252.2817	252.2815
	$C_{33}H_{62}O$	474.4801	474.4798
	$C_{33}H_{66}$	462.5165	462.5162
	$C_{33}H_{62}O$	474.4801	474.4795
	$C_{33}H_{66}$	462.5165	462.5156
	$C_{45}H_{50}O_7$	702.3557	702.3553
	$C_{45}H_{90}$	630.7043	630.7024

4. Life-cycle greenhouse gas assessment
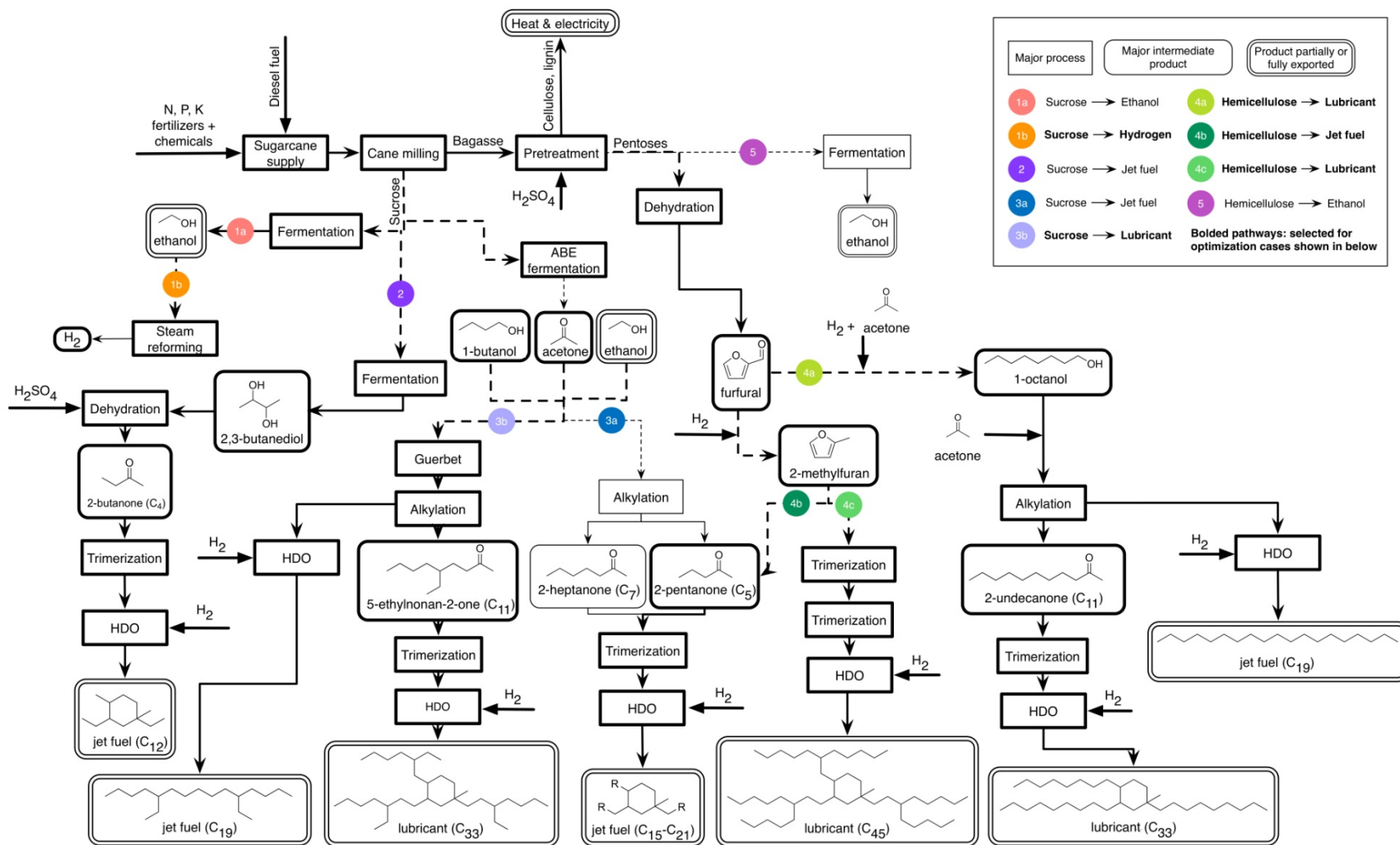
Fig. S30. Process flow diagram for hypothetical biorefinery, including all possible conversion processes.

We used life-cycle assessment (LCA) to quantify the net greenhouse gas (GHG) footprint of the fuel production scheme presented in our paper. The feedstock used for analysis was Brazilian sugarcane and conversion processes were modeled using a combination of existing chemical process models, proprietary models, and simplifying assumptions where necessary. Our model is run for a hypothetical facility that processes 5 million wet tonnes of sugarcane annually, although we assume inputs scale approximately linearly with size. Data sources for material and energy inputs as well as methodological choices are outlined here. For specific pathways, refer to Fig. S30. Total annual GHG emissions data are provided in Table S5.

Feedstock and cane milling

We assume the Brazilian sugarcane feedstock is cultivated in the southern part of Brazil, in the states of São Paulo and Minas Gerais, where a large fraction of current sugarcane cultivation and ethanol production is concentrated. Our crop input and yield data is largely drawn from national survey data reported in article by Seabra and Macedo (7). Process data for cane milling, including sugar and bagasse yield are also taken from Seabra and Macedo (7). We assume sugarcane vinasse is returned to the sugarcane field to restore nutrients to the soil and sugarcane is mechanically harvested. Table S4 shows the key data inputs.

Heat and power needs and production

Brazilian sugarcane biorefineries burn bagasse to supply the process heat and electricity required by the facility, with excess electricity exported to the grid. Seabra and Macedo (7) report that the average surplus generation in 2008 was 10.7 kWh/tonne of cane input, and the average for only facilities that sell power to the grid was 25 kWh/tonne cane. Traditional sugarcane biorefineries require approximately 30 kWh/tonne cane to operate, meaning that half of total electricity production is exported. Two factors are expected to drive net heat production and power exports in the coming decades: 1) the phasing out of on-field trash burning and manual harvest in favor of mechanical harvesting, in which the trash (mass equivalent to approximately half that of bagasse) will be collected for use as additional fuel, and 2) the installation of high-pressure boilers in new facilities, which will increase the efficiency of on-site energy production. Seabra and Macedo (7) estimate that these changes will result in greater than a factor of five increase in total electricity exports, totaling 130 kWh/tonne cane, and substantially increased process heat supply.

Another factor that impacts the importance of net electricity exports in Brazil is the country's grid mix. Estimates of Brazil's electricity mix in the literature and popular tools such as GREET and CA-GREET are remarkably inconsistent, ranging from 55% to 85% hydroelectricity. Furthermore, the marginal mix, which is meant to represent the combination of power sources that ramp up to meet a small increase in power demand or ramp down if demand decreases, is considered to be identical to the average mix in GREET, while CA-GREET assumes that 100% of marginal power is supplied by natural gas-fired plants. According to the January 2015 report from Brazil's Ministério de Minas e Energia, installed capacity is as

follows: 66.6% hydro, 9.5% natural gas, 9.2% biomass, 6.8% fuel oil, 3.7% wind, 2.7% coal, 1.5% nuclear (8). During the wet season, hydro supplies 76% Brazil's total power (9). Hydro's contribution drops to 67% of power during the dry season, while gas and oil-fired electricity generation increases (10). Conversely, sugarcane harvest and milling occurs during the dry season, when bagasse-fired power supplies 6% of power, and this contribution drops by an order of magnitude during the wet season, when sugarcane facilities are not operating (9, 10).

Because this article seeks to assess whether the drop-in fuels presented here will achieve the required GHG emissions reductions under current regulations, we have chosen to use a marginal electricity mix for Brazil that is consistent with GREET's assumptions: 83% hydroelectricity, 5% natural gas, 1.2% petroleum, 1.7% coal, 4.2% biomass, and 3.0% nuclear (11). However, the data we present here shows that this is unlikely to be an accurate representation of the electricity sources displaced by increasing biomass-fired power exports. Instead, the marginal mix displaced by biorefinery power exports is more likely to be comprised of gas and, secondarily, oil power plants, based on the reported seasonal variations in power generation. If biorefineries choose to employ storage methods for biomass, allowing them to generate and export power during the wet season, this may alter the displaced power mix. Conservatively, we assume in this study that facility-wide power demand is 50% greater per tonne of cane input than the power requirements for an ethanol-only facility.

The heat and power needs for our modeled sugarcane biorefinery are uncertain; we hope to improve these estimates in subsequent studies through a combination of additional experiments and process modeling. However, the already-abundant bagasse supply (minus hemicellulose, which we assume is used for fuel production) plus the newly-available sugarcane trash and improved efficiency of high-pressure boilers are indications that, unless the energy demands for our modeled biorefinery are greater than a five times that of a traditional ethanol facility, the on-site biomass should serve as a sufficient energy supply. For reference, using a lower heating value of 18 MJ/kg of dry biomass and 185 kg of dry biomass yield (cellulose and lignin fractions of bagasse plus trash), approximately 2600 MJ of thermal energy is available, minus the amount used for drying the biomass and efficiency losses. In comparison, our model suggests that one tonne of cane could yield 64.4 kg ABE (acetone, butanol, and ethanol) and up to 18 kg of furfural as intermediates. The modeled thermal energy required to extract the ABE and furfural intermediates from solution is 5.5 MJ/kg and 4.1 MJ/kg, respectively, leading to a total thermal energy requirement of approximately 130 MJ per tonne of cane. As is clear from these simple calculations, the thermal energy needs are unlikely to exceed the energy that residual biomass can provide.

Burning additional biomass for process heat beyond what is required in traditional Brazilian sugarcane facilities will not appreciably impact the GHG balance because the carbon released is biogenic. Furthermore, variations in power exports have a minor impact on the overall GHG footprint of the fuels because the mix of power displaced is largely carbon-neutral. However, as discussed earlier, the standard method of calculating power-related carbon offsets is

not necessarily reflective of actual power offsets. We explore the sensitivity of the results further in the *Uncertainty and Sensitivity* section below.

Biorefining

Although the majority of biorefining inputs and outputs are drawn from either Seabra and Macedo (7) or the schemes documented in our paper, some addition inputs such as lime input for flue gas desulfurization and sulfuric acid neutralization were calculated based on a combination of proprietary Aspen Plus models and models released by the National Renewable Energy Laboratory (NREL). We assume that lime required for flue gas desulfurization is correlated with the quantity of sulfuric acid utilized during pretreatment, using the model documented in Humbird et al. (12) as a base case. For wastewater treatment, we utilize overliming as consistent with Aden et al. (13), although we choose to use $CaCO_3$ as an input rather than hydrated lime. We assume that the quantity of lime required for neutralization of sulfuric acid is linearly correlated with the input quantity of sulfuric acid, meaning no lime is required if bagasse is not treated with sulfuric acid.

Transportation

We assume that both alkanes and ethanol must be transported 700 km by tanker truck before reaching terminals where they can be transferred to marine tankers. We then assume all fuel is transported 1000 km by marine tanker to international markets.   Although these assumptions are fairly arbitrary, the results are largely insensitive to transportation distances. Sugarcane transportation distances are taken from national survey data in Seabra and Macedo (7).

Pathway 1a and 1b: Sucrose fermentation to ethanol and steam reforming

Our assumed ethanol yield from the fermentation of cane sugar is 1900 MJ ethanol per wet tonne of cane (shown in Table S4). This ethanol can either be sold entirely as fuel, or reformed to produce hydrogen needed elsewhere in the biorefinery. We use 90% selectivity for hydrogen production via steam reforming of ethanol based on data from Haryanto et al. (14).

Pathway 2: Sucrose conversion to jet fuel via BDO

28
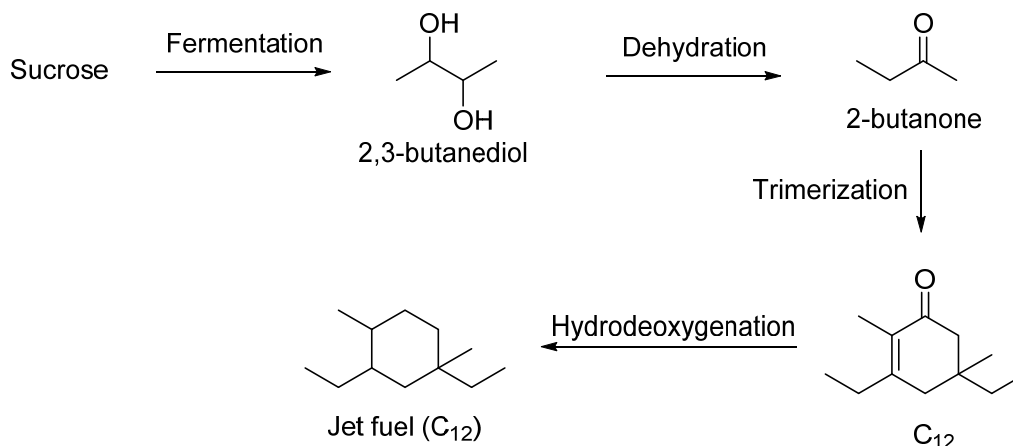
We use data for fermentation of sucrose to 2,3-butanediol by *S. marcescens* from Zhang et al (15), yielding 0.47 g of BDO per g of sucrose. All additives for this process are assumed to be recyclable. BDO is then converted to methyl ethyl ketone (MEK) using a sulfuric acid catalyst with a 93% yield (16). MEK is trimerized and hydrodeoxygenated to produce the final jet fuel product; we assume a 95% selectivity for trimerization and 3 mol of H_2 required per mol of trimer, with a 10% loss rate during H_2 recycling. Total hydrogen needs for the process are 1 kg of H_2 per 100 kg of sucrose converted. 15.6 kg of H_2SO_4 are required per 100 kg of sucrose converted, which we assume is not recycled, but rather neutralized with NaOH and disposed.

ABE fermentation

For fermentation of cane sugar to acetone, 1-butanol, and ethanol by *Clostridium acetobutylicum*, we use the conventional yield ratio of 3:6:1, and a total mass yield of 0.46 kg liquid products/kg glucose or fructose. Hydrogen yield is assumed to be 0.021 kg of H_2 per kg glucose or fructose. These data are based on GREET data and based on the assumption that sucrose-derived fructose is converted at a similar rate to glucose (17). For both pathways (3a and 3b) that rely on ABE fermentation, we treat 1-butanol as the limiting reactant, with the expectation that both acetone and ethanol can either be purchased or produced elsewhere in the biorefinery.

Pathway 3a: Jet fuel via ABE fermentation of cane sugar
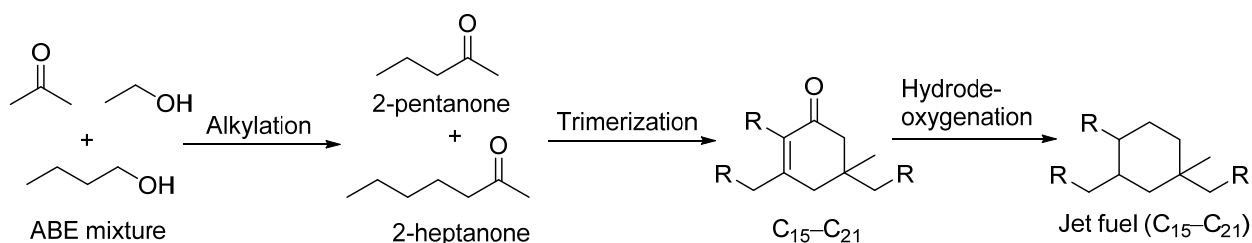
Production of jet fuel via ABE fermentation of cane sugar requires all three products: acetone, 1-butanol, and ethanol, although not in the exact ratio in which they are produced. Acetone, 1-butanol, and ethanol undergo alkylation to produce 2-heptanone and 2-pentanone. Acetone yield from fermentation is approximately half that of 1-butanol, but for each kg of 1-butanol processed, 0.78 kg of acetone are required. This means acetone must either be supplied internally or fossil-derived acetone can be imported. Conversely, more than enough hydrogen to meet the process' needs is produced as a co-product of fermentation, allowing for excess hydrogen to be used elsewhere in the biorefinery. For each kg of 1-butanol input, this process yields 50 MJ of jet-range fuel, assuming all acetone and ethanol needs are met.

Pathway 3b: Lubricant via ABE fermentation of cane sugar

This process requires both acetone and 1-butanol; ethanol is not required and can be exported as fuel or used elsewhere in the biorefinery. 1-Butanol undergoes a Guerbet reaction at 90% selectivity to 2-ethylhexanol, followed by an alkylation reaction with acetone to produce 2-

undecanone (C_{11} compound) at 90% selectivity. The remaining 10% results in a C_{19} compound and that can be hydrodeoxygenated and sold as jet fuel. Unlike Pathway 3a, which requires acetone beyond what is produced via fermentation, this pathway only requires 0.37 kg acetone per kg 1-butanol input (as compared to 0.5 kg acetone/kg 1-butanol produced via fermentation). The C_{11} precursor is then trimerized and hydrodeoxygenated to produce a C_{33} lubricant. Total hydrogen production via ABE fermentation exceeds the hydrogen needs of the process, indicating that Pathway 3b could be effectively paired with pathways that are net consumers of hydrogen and acetone. For each kg of 1-butanol input to the process, 0.76 kg of lubricant are ultimately produced.
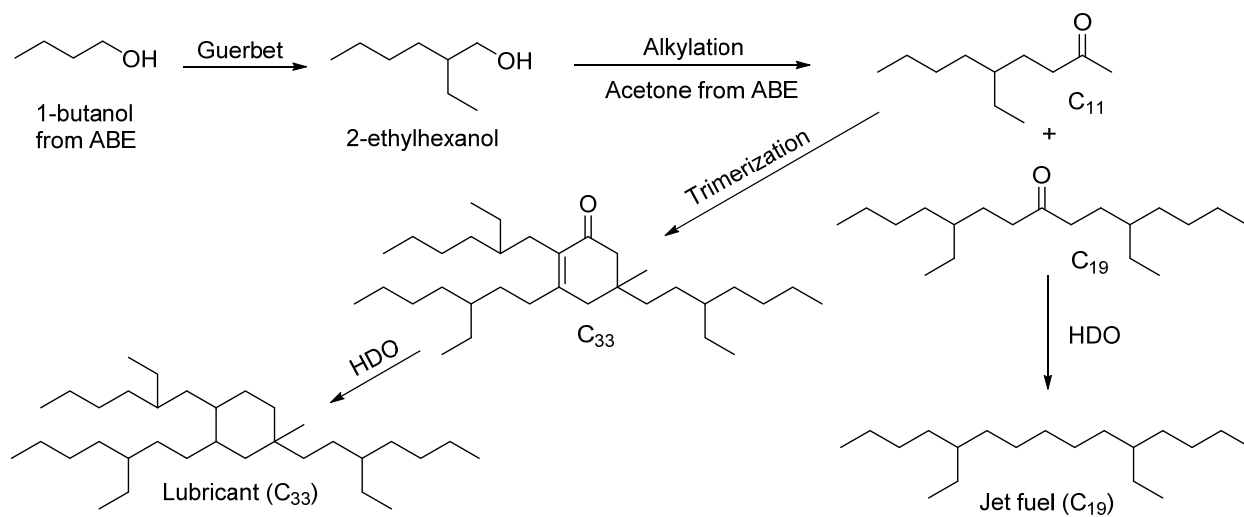
Pathway 4a: Lubricant from hemicellulose via octanol

Each hemicellulose conversion pathway begins with dehydration of pentose sugars using sulfuric acid to produce furfural. We assume xylan is converted to xylose with 90% selectivity (12), and xylose is converted to furfural at 90% selectivity (18). Sulfuric acid from pretreatment, during which cellulose and lignin are separated for combustion, can be reused for the dehydration reaction to convert xylose to furfural. Pathway 4a requires hydrogen and acetone to produce furfuralacetone, which is converted to 1-octanol at 90% selectivity (19). 1-Octanol undergoes alkylation with acetone to produce 2-undecanone (a C_{11} precursor) at 87% selectivity (based on experimental results), which can be trimerized and hydrodeoxygenated to produce a C_{33} lubricant. The remaining 13% of the alkylation products can be converted to C_{19} jet fuel in the same manner described for Pathway 3b. For each bone dry kg of hemicellulose input, 0.57 kg of lubricant are yielded; this yield appears high in large part because of the large acetone inputs, which must either be purchased or provided through other processes within the biorefinery.
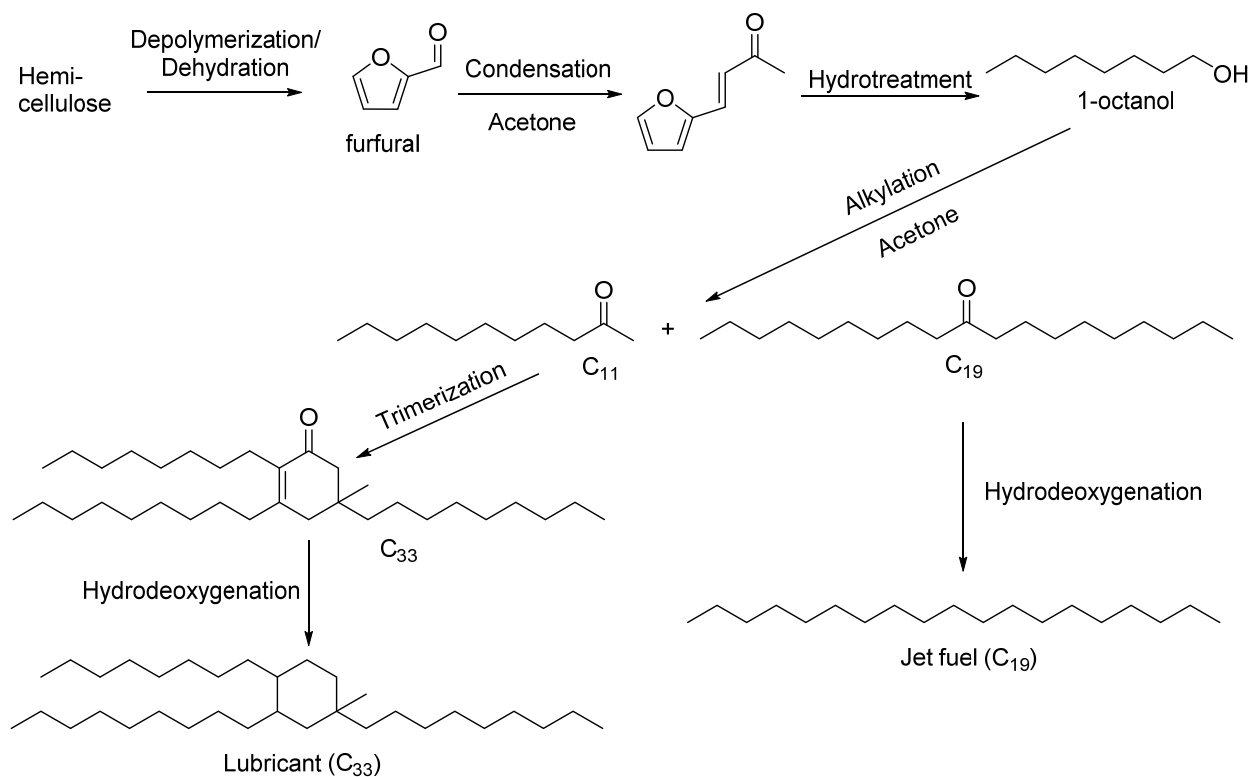
Pathway 4b: Jet fuel from hemicellulose via 2-methylfuran

Using hemicellulose-derived furfural as a starting material (see Pathway 4a description for furfural yield), 2-methylfuran (2-MF) and subsequently 2-pentanone can be produced via hydrotreatment at near-stoichiometric yields (20). The 2-pentanone then undergoes the process described in Pathway 3a, yielding 14 MJ of jet fuel per kg of bone dry hemicellulose input. This pathway does not require any inputs aside from heat/power and hydrogen.
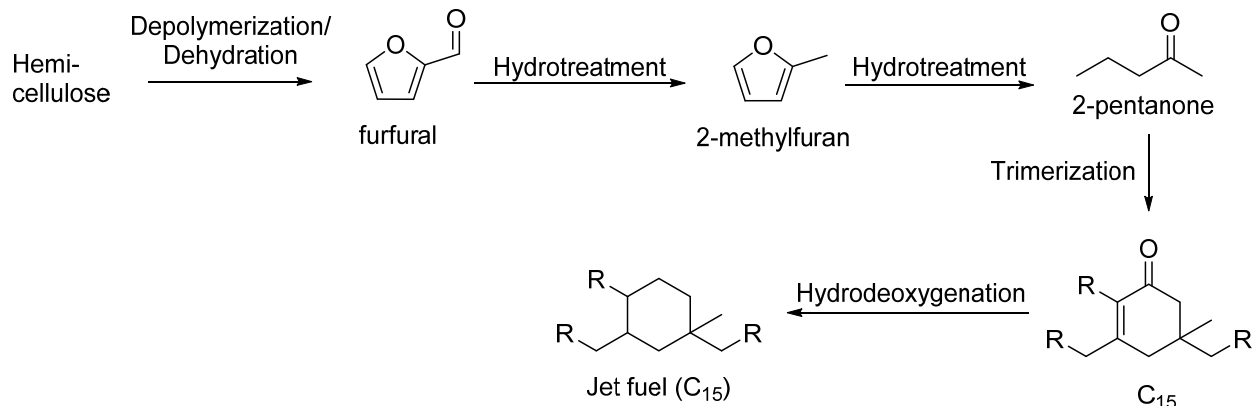
Pathway 4c: Lubricant from hemicellulose via 2-methylfuran

      Yields for 2-methylfuran are as described in Pathway 4b. 2-MF is then trimerized to produce a C_{15} precursor molecule at 94% selectivity (6). This C_{15} precursor is then trimerized to produce a C_{45} molecule that can be hydrodeoxygenated to produce the final lubricant. This pathway requires substantial hydrogen, but no acetone, in contrast to the competing hemicellulose-derived lubricant pathway (Pathway 4a). The final yield is 0.27 kg of lubricant for each kg of bone dry hemicellulose input.
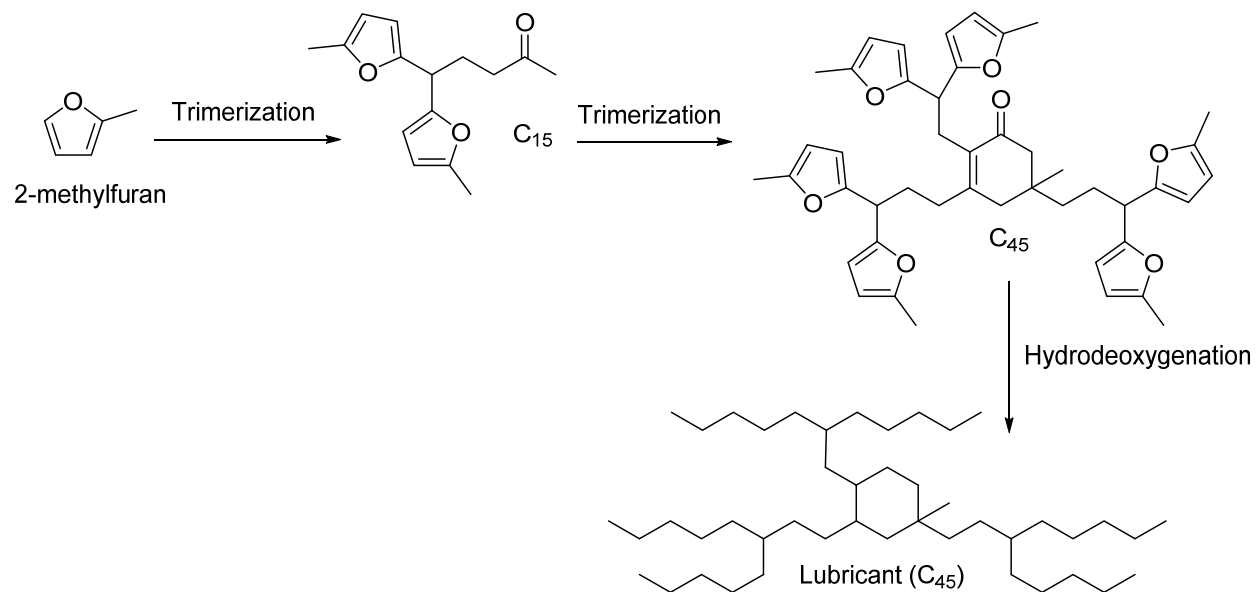
Pathway 5: Ethanol via fermentation of hemicellulose

For ethanol production via fermentation of hemicellulose, we use the same xylan conversion rate described in Pathway 4a. Final ethanol yield, based on data from Humbird et al. (12) is estimated to be 11 MJ per kg of hemicellulose input. As would be expected, no hydrogen or other inputs are required aside from heat and power.

Not included in optimization: Sucrose conversion to jet fuel via farnesene

This pathway is not included in the optimization, but is mentioned in the manuscript as a comparable drop-in fuel pathway. In this case, sucrose is converted to farnesene and hydrotreated to produce farnesane, which can be used directly as jet fuel. We use a range of yields between 0.168 kg farnesene/kg sucrose and 0.26 kg farnesene/kg sucrose (21). 4 mol of H_2 are then required per mol of farnesene to convert farnesene into farnesane, with a 10% loss during recycling. We completed the life-cycle GHG inventory based on the assumption that all necessary hydrogen is produced via steam-reforming of natural gas.

Optimization

All optimization results are based on our linear programming model, run in Matlab, which relies on the Simplex algorithm. The linear programming portion of our LCA/optimization model code, which is written in R and uses the R.matlab package to run the optimization in Matlab, is not shown here due to length limitation and is available from the authors by request.

Uncertainty and Sensitivity

The process input and yield assumptions described in previous sections are based on the best available data. Where possible, data was taken from literature documenting operations of commercial or pilot facilities. In cases where only bench-scale data was available, we recognize that these data may provide overly optimistic yields based on idealized conditions/feedstocks, or yields lower than what would eventually be achieved once the conversion technologies mature. However, in the absence of sufficient data regarding the uncertainty associated with each input value, assigning arbitrary ranges does not provide useful additional information.

As discussed in the main text, we conducted a sensitivity analysis to determine whether the optimization results differ if key input variables are adjusted. One highly uncertain variable is the fraction of lubricants that are repurposed as a component in asphalt at their end-of-life, currently assumed to be 10%; we found that the optimal pathway combinations remain unchanged even if the fraction of lubricants sequestered is reduced to zero and the maximum net reduction in GHG emissions relative to petroleum products is reduced from 81% to 75%. Another important variable is the furfural yield from C_5 sugars. Although an HCl acid catalyst results in a higher yield (90%), we found that producing HCl for use at a rural sugarcane facility is energy- and GHG-intensive. If H_2SO_4 can be used to achieve a yield of 70%, that choice is preferable because the acid can, at least in part, be reused from the pretreatment step and H_2SO_4 is less energy-intensive to produce. If the furfural yield drops below 60%, our optimization

results change dramatically: minimizing emissions results in all sucrose and hemicellulose being allocated to ethanol production because the acetone and hydrogen needs/demands can no longer be balanced.

Another important source of uncertainty is the assumed mix of electricity that is displaced by increasing biorefinery power exports. We conduct a sensitivity analysis by varying the amount of electricity exported from the biorefinery and the mix of grid electricity that is offset. These ranges are reflected in the error bars for Fig. 3. In the "high" case, the biorefinery uses 2.5 times the electricity of a comparably sized traditional ethanol facility and the net electricity usage is met entirely by natural gas simple cycle power. In the "low" case, the biorefinery uses only 25% more power than a traditional ethanol facility and net electricity exports offset entirely natural gas simple cycle power. Our base case, for comparison, uses an electricity mix that is primarily hydro and assumes that the biorefinery uses 50% more electricity than a typical ethanol facility.

Table S4. Data and assumptions for LCA calculations.

Process	Operating parameter		Unit	Data source
Sugarcane cultivation	Diesel input	115	MJ/wet tonne cane	Seabra et al. (7)
	Nitrogenous fertilizer input	0.78	kg N/wet tonne cane	Seabra et al. (7)
	P_2O_5 input	0.25	kg/wet tonne cane	Seabra et al. (7)
	K_2O input	0.98	kg/wet tonne cane	Seabra et al. (7)
	$CaCO_3$ input	5.2	kg/wet tonne cane	Seabra et al. (7)
	Atrazine	0.048	kg/wet tonne cane	GREET (11)
Cane transportation	Flatbed truck	21	km	Seabra et al. (7)
Cane milling	Sucrose yield	140	kg/wet tonne cane	Seabra et al. (7)
	Bagasse yield	0.28	wet tonne/wet tonne cane	Seabra et al. (7)
Sucrose fermentation	Ethanol yield	1900	MJ/wet tonne cane	Seabra et al. (7)
Pretreatment	Sulfuric acid input	5	kg/wet tonne cane	Calculated
Power generation	Total generation (base case)	66	kWh/wet tonne cane	Calculated
	Onsite use (base case)	21	kWh/wet tonne cane	Calculated

	Net export (base case)	45	kWh/wet tonne cane	Calculated
	FGD lime input	3.9	kg/wet tonne cane	Calculated
BDO from sucrose	Yield	0.47	kg/kg sucrose	Zhang et al. (15)
MEK from BDO	Yield	93%	--	Emerson et al. (16)
ABE fermentation	Total mass yield	0.46	kg/kg glucose & fructose	Wu et al. (17)
	Acetone:butanol:ethanol ratio	3:6:1	--	Wu et al. (17)
Furfural from hemicellulose	Xylan to xylose conversion	85%	--	Humbird et al. (12)
	Xylose to furfural conversion	70%	--	SupraYield process
Wastewater treatment	$CaCO_3$ input	5	kg/wet tonne cane	Calculated
Liquid product transportation	Tanker truck	700	km	Assumption
	Marine tanker	1000	km	Assumption
Conventional fuels/lubes GHG footprints	Gasoline	95		CA LCFS
	Jet fuel	90		Bailis & Baka (22)
	PAO lubricant	87		Calculated, based on 25% sequestration Johnson et al. (23)

Table S5. Annual life-cycle greenhouse gas emissions results for 5 million wet tonnes/year sugarcane biorefinery (g CO_2-equivalent/MJ output).

Product/sector/activity	Sucrose → ethanol	Sucrose → BDO → jet fuel	Sucrose → ABE → jet fuel	Sucrose → ABE → lubricant
Atrazine	0.213040055	0.239890735	0.196157502	0.246344422
Lime	0.928427051	1.045442124	0.854853008	1.073567248
$CaCO_3$	0.665775938	0.749687561	0.613015921	0.769856114
H_2SO_4	0	0.030238767	6.65E-06	-3.92E-06
HCl	0	0	0	0
NaOH	0	11.94350696	0	0
K_2O	0.150239319	0.169174856	0.138333468	0.173726102
N Fertilizer	2.467817455	2.778850874	2.272253023	2.853609219
P_2O_5	0.043963979	0.049505016	0.040480014	0.05083683
Coal	0.002094535	0.021325559	0.004285658	0.000834571
Diesel	1.293074591	1.284948252	1.10740259	1.273667747

RFO	0.014119043	0.014079978	0.011294475	0.00957406
Propene	0	0	0.568250395	-0.335024352
Acetone	0	0	0.511060904	-0.301307046
Crude Oil	0.141193064	0.140347026	0.314640388	0.022503416
US Electricity Mix	0.717490398	11.65904667	2.061220355	-0.113575445
Natural Gas Simple Cycle Power	-0.700204643	-0.788455516	-0.644716291	-0.809667028
NGCC Power	-1.120328252	-1.261529753	-1.031546824	-1.295468197
US WECC Electricity Mix	1.72E-05	0.000280051	4.95E-05	-2.73E-06
US MRO Electricity Mix	1.23E-05	0.000199547	3.53E-05	-1.94E-06
Gasoline	1.75E-05	0.000178261	1.202552498	-0.708962825
H_2 via Natural Gas Reforming	0	10.52201087	0	0
Natural Gas	0.004947914	0.955651749	0.123801849	-0.07425335
Uranium	2.40E-05	0.000389848	6.89E-05	-3.80E-06
Brazilian Cane Cultivation	9.977772213	11.23532901	9.187074608	11.5375887
Farm Equipment	0.130126924	0.146527579	0.119814898	0.150469554
Flatbed Truck Transportation	1.832190656	2.10559515	1.69227655	2.115059935
Tanker Truck Transportation	4.050099379	2.890681402	2.940641696	2.891777592
Gas Pipeline Transportation	0.003715468	0.717614244	0.092964796	-0.055758032
Rail Transportation	0.063134492	0.223105154	0.130817605	0.023061816
Barge Transportation	0.008465976	0.026989927	0.018497313	0.001832649
Marine Tanker Transportation	0.558062855	0.374959609	0.440543067	0.380747814
Direct Biorefinery Emissions	0	0	12.31108465	0
Lube CO_2 Sequestration	0	0	0	-6.836509695

Product/sector/activity	Hemicellulose → ethanol	Hemicellulose → octanol → lubricant	Hemicellulose → 2-MF → jet fuel	Hemicellulose → 2-MF → lubricant
Atrazine	0.178699186	0.145057382	0.172196631	0.178033124
Lime	0.496731546	0.403217156	0.478656342	0.49488009
$CaCO_3$	0.825042328	0.669720342	0.795020461	0.821967167
H_2SO_4	0.005646974	0.004591383	0.00544149	0.005625926
HCl	0	0	0	0
NaOH	0	0	0	0
K_2O	0.126021578	0.10229683	0.121435871	0.125551861
N Fertilizer	2.070019039	1.680318467	1.994694618	2.062303506
P_2O_5	0.036877231	0.029934745	0.035535332	0.036739779
Coal	0.001584201	0.004218544	0.001691731	0.00172908
Diesel	1.185017087	1.053393227	1.126918297	1.159878516

RFO	0.014011657	0.014768211	0.013078958	0.013371553
Propene	0	0.64144728	0	0
Acetone	0	0.576891155	0	0
Crude Oil	0.129920364	0.335741696	0.123430161	0.126996088
US Electricity Mix	0.659328939	2.277739894	0.733484879	0.74646739
Natural Gas Simple Cycle Power	-0.211273537	-0.171499304	-0.203585657	-0.210486062
NGCC Power	-0.338037907	-0.274399089	-0.325737291	-0.336777946
US WECC Electricity Mix	1.58E-05	5.47E-05	1.76E-05	1.79E-05
US MRO Electricity Mix	1.13E-05	3.90E-05	1.26E-05	1.28E-05
Gasoline	1.32E-05	1.357449277	1.41E-05	1.45E-05
H_2 via Natural Gas Reforming	0	6.249416047	8.068998164	7.601882702
Natural Gas	0.117617689	0.596218472	0.576990191	0.55375455
Uranium	2.20E-05	7.62E-05	2.45E-05	2.50E-05
Brazilian Cane Cultivation	8.369410959	6.793790553	8.064862536	8.338215853
Farm Equipment	0.10915119	0.088602451	0.105179366	0.108744353
Flatbed Truck Transportation	1.536464903	1.253779393	1.480925564	1.531075805
Tanker Truck Transportation	4.052085014	3.944056525	3.778604313	3.863124346
Gas Pipeline Transportation	0.088321011	0.447710024	0.433271199	0.415823183
Rail Transportation	0.076742176	0.149463415	0.073897321	0.076233655
Barge Transportation	0.007458879	0.019395624	0.00726645	0.007465255
Marine Tanker Transportation	0.554064029	0.57774706	0.516715236	0.528287893
Direct Biorefinery Emissions	0.979852558	14.69227351	0.944197414	0.976200377
Lube CO_2 Sequestration	0	-2.427013042	0	-1.428373679

Product/sector/activity	Optimization A	Optimization B	Optimization C
Atrazine	0.178667046	0.220603992	0.185381342
Lime	0.496642206	0.613214668	0.51530599
$CaCO_3$	0.82489394	1.018514048	0.855893403
H_2SO_4	0.005645958	0.029782947	0.005858133
HCl	0	0	4.75E-05
NaOH	0	9.010038234	0.180908918
K_2O	0.125998913	0.155573531	0.130733944
N Fertilizer	2.069646736	2.555436733	2.147423932
P_2O_5	0.036870598	0.04552491	0.038256193
Coal	0.001510439	0.016013665	0.001976211
Diesel	1.084240422	1.228057748	1.083177161
RFO	0.011126136	0.012886785	0.010411236

Propene	-1.31E-08	0	-1.04E-14
Acetone	-1.18E-08	0	-9.37E-15
Crude Oil	0.118039972	0.133849618	0.117579255
US Electricity Mix	0.615550607	8.851033701	0.861309062
Natural Gas Simple Cycle Power	-0.211235538	-0.260817	-0.219173756
NGCC Power	-0.337977109	-0.417307507	-0.350678268
US WECC Electricity Mix	1.48E-05	0.000212603	2.07E-05
US MRO Electricity Mix	1.05E-05	0.000151487	1.47E-05
Gasoline	1.26E-05	0.000133859	1.91E-05
H_2 via Natural Gas Reforming	7.69E-08	0	8.99E-13
Natural Gas	0.114002674	0.401514931	0.129403458
Uranium	2.06E-05	0.000295955	2.88E-05
Brazilian Cane Cultivation	8.367905678	10.33203067	8.682371058
Farm Equipment	0.109131558	0.13474705	0.113232715
Flatbed Truck Transportation	1.536023987	1.928251989	1.594663785
Tanker Truck Transportation	3.212840949	2.86176627	2.981058711
Gas Pipeline Transportation	0.085606439	0.301504009	0.097171134
Rail Transportation	0.074094046	0.206310103	0.077449811
Barge Transportation	0.006845444	0.021566121	0.007273999
Marine Tanker Transportation	0.439589628	0.372654748	0.407860429
Direct Biorefinery Emissions	0.979676326	1.209627144	1.016492502
Lube CO_2 Sequestration	-4.114344372	0	-6.799358832

5. References:

1. Eddings EG, Yan S, Ciro W, Sarofim AF (2005) FORMULATION OF A SURROGATE FOR THE SIMULATION OF JET FUEL POOL FIRES. *Combust. Sci. Technol.* 177(4):715-739.
2. Wasserscheid P, Grimm S, Köhn Randolf D, Haufe M (2001) Synthesis of Synthetic Lubricants by Trimerization of 1-Decene and 1-Dodecene with Homogeneous Chromium Catalysts. *Adv. Synth. Catal.* 343(8):814-818.
3. Anonymous (2012) Engine Oil Licensing and Certification System, API 1509, 17th edition. (American Petroleum Institute, 1220 L Street, N.W., Washington, D.C. 20005, USA.).
4. Xu W, et al. (2011) Effective Production of Octane from Biomass Derivatives under Mild Conditions. *ChemSusChem* 4(12):1758-1761.
5. Mori K (2010) New Syntheses of 1,7-Dimethylnonyl Propanoate, the Western Corn Rootworm Pheromone, in Four Different Ways via Cross Metathesis, Alkylation and Coupling Reactions. *Biosci. Biotechnol. Biochem.* 74(3):595-600.
6. Corma A, de la Torre O, Renz M, Villandier N (2011) Production of High-Quality Diesel from Biomass Waste Products. *Angew. Chem. Int. Ed.* 50(10):2375-2378.

7.   Seabra JEA, Macedo IC (2011) Comparative analysis for power generation and ethanol production from sugarcane residual biomass in Brazil. *Energy Policy* 39(1):421-428.

8.   Anonymous (2015) Boletim Mensal de Monitoramento do Sistema Elétrico Brasileiro, Janeiro 2015.

9.   Anonymous (2014) Boletim Mensal de Monitoramento do Sistema Elétrico Brasileiro, Março 2014.

10.   Anonymous (2014) Boletim Mensal de Monitoramento do Sistema Elétrico Brasileiro, Setembro 2014.

11.   Anonymous (2012) GREET Fuel Cycle Model. (Argonne National Laboratory, Argonne, IL).

12.   Humbird D, et al. (2011) Process Design and Economics for Biochemical Conversion of Lignocellulosic Biomass to Ethanol. (National Renewable Energy Laboratory, Golden, CO).

13.   Aden A, et al. (2002) Lignocellulosic Biomass to Ethanol Process Design and Economics Utilizing Co-Current Dilute Acid Prehydrolysis and Enzymatic Hydrolysis for Corn Stover. (National Renewable Energy Laboratory, Golden, CO).

14.   Haryanto A, Fernando S, Murali N, Adhikari S (2005) Current status of hydrogen production techniques by steam reforming of ethanol: A review. *Energy Fuels* 19(5):2098-2106.

15.   Zhang L, et al. (2010) Microbial production of 2,3-butanediol by a mutagenized strain of Serratia marcescens H30. *Bioresour. Technol.* 101(6):1961-1967.

16.   Emerson RR, Flickinger MC, Tsao GT (1982) Kinetics of dehydration of aqueous 2,3-butanediol to methyl ethyl ketone. *Industrial Engineering Chemistry, Product Research, and Development* 21(3):473-477.

17.   Wu M, Wang M, Liu J, Huo H (2007) Life-Cycle Assessment of Corn-Based Butanol as a Potential Transportation Fuel. (Argonne National Laboratory, Argonne, IL).

18.   Marcotullio G, De Jong W (2010) Chloride ions enhance furfural formation from d-xylose in dilute aqueous acidic solutions. *Green Chem.* 12(10):1739-1746.

19.   Julis J, Leitner W (2012) Synthesis of 1-Octanol and 1,1-Dioctyl Ether from Biomass-Derived Platform Chemicals. *Angew. Chem. Int. Ed.* 51(34):8615-8619.

20.   Corma A, Torr Odl, Ren M (2012) Production of high quality diesel from cellulose and hemicellulose by the Sylvan process: catalysts and process variables. *Energy & Environmental Science* 5(4):6328-6344.

21.   Pray T (September 29, 2010) Biomass R&D Technical Advisory Committee: Drop-in Fuels Panel (Available at: www.biomassboard.gov/pdfs/biomass_tac_todd_pray_09_29_2010.pdf). (Amyris, Aurora, Colorado).

22.   Bailis RE, Baka JE (2010) Greenhouse Gas Emissions and Land Use Change from Jatropha Curcas-Based Jet Fuel in Brazil. *Environmental Science & Technology* 44(22):8684–8691.

23.   Johnson MR, Reynolds JG, Love AH (2008) Improving Used Oil Recycling in California. (California Integrated Waste Management Board, Sacramento, CA).